Pharm Res (2013) 30:1677–1697
DOI 10.1007/s11095-013-1014-7

RESEARCH PAPER

Spray-Dried Chitosan Microparticles for Cellular Delivery of an Antigenic Protein: Physico-chemical Properties and Cellular Uptake by Dendritic Cells and Macrophages

Chirasak Kusonwiriyawong • Vimolmas Lipipun • Nontima Vardhanabhuti • Qiang Zhang • Garnpimol C. Ritthidej

Received: 13 July 2012 / Accepted: 15 February 2013 / Published online: 13 March 2013

ABSTRACT

Purpose Spray-dried chitosan microparticles for cellular delivery of antigen to dendritic cells (DC) and macrophages (Mφ) were investigated.

Methods Chitosan microparticles were prepared by spray drying. For comparison, poly(lactic-co-glycolic acid) (PLGA) and poly(α-butyl cyanoacrylate) (BCA) micro-/nanoparticles were generated. Bovine serum albumin (BSA) was used as a model antigen. The particles were characterized in terms of size, morphology, surface charge, surface composition, protein content, entrapment efficiency, *in vitro* release, and protein integrity. Additionally, they were subject to cell viability and cellular uptake study with DC and Mφ.

Results Size of chitosan, PLGA, and BCA micro-/nanoparticles ranged between 3.11–7.18, 0.94–6.26, and 0.30–6.34 μm, respectively. Particle morphology and *in vitro* protein release varied, depending on polymer type, particle composition and preparation process parameters. Chitosan microparticles were cationic, while PLGA microparticles were neutral. BCA micro-/nanoparticles were either anionic or cationic, according to polymerization pH. Protein content and entrapment efficiency of chitosan and PLGA microparticles were relatively consistent. Only integrity and conformational structure of protein encapsulated in chitosan microparticles were completely retained. Chitosan and PLGA microparticles were non-toxic to DC and Mφ, but the former were internalized more efficiently.

Conclusions Spray-dried chitosan microparticles delivered the antigen efficiently to DC and Mφ.

KEY WORDS cellular uptake · chitosan microparticles · dendritic cell · macrophage · spray dry

ABBREVIATIONS

BCA	Poly(α-butyl cyanoacrylate)
BSA	Bovine serum albumin
C	Cross-linked microparticles
CD	Circular dichroism
CLSM	Confocal laser scanning electron microscope
D	Dextran
DC	Mouse dendritic cells
EUD	Poly(butyl methacrylate-co-[2-dimethyl aminoethyl] methacryalte-co-methyl methacrylate 1:2:1) (Eudragit EPO)
FACS	Fluorescent-activated cell sorter
FITC	Fluorescein-5-isothiocyanate isomer I
GEL	Gelatin
HCS	Chitosan (100 kDa) of Thailand
JCS	Chitosan (50–100 kDa) of Japan

C. Kusonwiriyawong • N. Vardhanabhuti • G. C. Ritthidej (✉)
Department of Pharmaceutics and Industrial Pharmacy
Faculty of Pharmaceutical Sciences, Chulalongkorn University
Bangkok 10330, Thailand
e-mail: garnpimol.r@chula.ac.th

V. Lipipun
Department of Biochemistry and Microbiology
Faculty of Pharmaceutical Sciences, Chulalongkorn University
Bangkok 10330, Thailand

Q. Zhang
Department of Pharmaceutics, School of Pharmaceutical Sciences
Peking University, Beijing 100083, People's Republic of China

Present Address:
C. Kusonwiriyawong
Faculty of Pharmacy, Rangsit University, Pathum Thani 12000, Thailand

LC_{50}	Lethal particle concentration providing a decrease of 50% cell survival
LCS	Chitosan (37 kDa) of Thailand
Mφ	Spleenic mouse macrophages
PBS	pH7.4 Phosphate buffered saline
PLGA	Poly(lactic-co-glycolic acid)
POL	Poloxamer 407 (Lutrol F 127)
PVA	Poly(vinyl alcohol)
XPS	X-ray photoelectron spectroscopy

INTRODUCTION

Many biopharmaceuticals, both peptide-/protein-based and nucleic acid-based, need to be trafficked into the correct intracellular compartment, in order to bind with their targets and subsequently express their activity. For example, DNA first needs to escape endosomal compartment before it can enter into further steps towards transcription to the encoded proteins. Similarly, antisense oligonucleotides must reach distinct compartments inside the cell, such as the cytosol and/or nucleus, and interact with the target mRNA to exhibit an antisense effect. Furthermore, the delivery of exogenous antigens to professional antigen presenting cells is mandatory for vaccine therapeutics. To fulfill these purposes, efficient delivery systems are essentially needed.

Numerous polymeric micro-/nanoparticles have shown a certain degree of success for delivery of drugs and proteins to the systemic circulation or target site (1,2). Of those, the biodegradable and biocompatible synthetic polyesters, especially poly(lactic acid) and poly(lactic-co-glycolic acid) (PLGA), are the primary candidates for the development of microparticles for vaccine adjuvants or delivery systems (3–7), since they have been used in humans for many years as resorbable suture materials and as controlled release drug delivery systems (1). Other synthetic polyesters used for preparation of particulate delivery systems include poly(ε-caprolactone) (8–10) and poly (alkyl cyanoacrylate) (11–13). Traditionally, these particles are generated by emulsification of two or more immiscible liquid phases, followed by solidification, which subsequently leads to the entrapment of drugs and proteins into the particles (1,14). The application of organic solvents and surfactants as well as high shear force, usually produced by homogenization or ultrasonication, during the preparation process has been reported to impose deleterious effects on conformational structure of encapsulated proteins (15–18), which will evidently reduce the enzymatic activity and/or the antigen immunogenicity. Furthermore, the encapsulation efficiency of drugs and proteins within the particle matrix is rather low, due to leakage of the internal aqueous phase into the external aqueous phase upon emulsification (14).

Chitosan is a polysaccharide composed of D-glucosamine and trace amount of N-acetyl-D-glucosamine, derived from the exoskeleton of crustaceans. It has been recognized as a promising material for delivery of drugs and labile macromolecular compounds, attributed to its excellent biocompatibility and biodegradability (19). In addition, it is important to note that chitosan is soluble in mildly acidic aqueous solution and, therefore, does not require organic solvents in its formulation and subsequent preparation of micro-/nanoparticles (20), which is an obvious advantage over other synthetic polymers.

Microparticulate carriers offer several attributes for use as antigen delivery systems. These include protection of antigens encapsulated in microparticles from extracellular enzymatic degradation and controlled release of entrapped antigens, allowing a possible single-injection vaccine formulation (21). Of critical importance, microparticles have a similar size to the pathogens (<5 μm) that the immune system has evolved to combat. As a consequence, they are efficiently internalized by antigen presenting cells (22), in particular, DC and Mϕ. It is largely believed that the effective uptake of particulate antigen delivery systems into and subsequent stimulation of antigen presenting cells are fundamental in the induction of innate and adaptive immune response through major histocompatibility complex class I and class II pathways (23,24).

This study was aimed to investigate the potential of spray-dried chitosan microparticles as antigen delivery systems for passive targeting to antigen presenting cells. Selected excipients were co-spray dried with chitosan in order to produce chitosan composite microparticles, with desired properties and/or possibly improved cellular uptake. Bovine serum albumin (BSA) was used as a model antigenic protein. The microparticles were characterized in terms of various physicochemical properties, including size, morphology, surface charge, surface composition, protein content, entrapment efficiency, *in vitro* release, and protein integrity. Additionally, their biological properties were characterized, especially the cellular uptake into DC and Mϕ, which was an important prerequisite to the initiation of effective immunity. For comparison, PLGA and Poly(α-butyl cyanoacrylate) (BCA) micro-/nanoparticles were also prepared and investigated.

MATERIALS AND METHODS

Materials

Chitosan at molecular weight of 37 kDa with 94% degree of deacetylation (LCS) and 100 kDa with 95% degree of deacetylation (HCS) were obtained from Seafresh Chitosan (Bangkok, Thailand). Chitosan of different source (Flonac™ C, molecular weight of 50–100 kDa and 90.7% degree of deacetylation) (JCS) was provided by Kyowa Technos (Chiba, Japan). BSA, Cohn Fraction V was purchased from Sigma-Aldrich (Singapore). Gelatin (GEL) was supplied by Fluka Chemie (Buchs, Switzerland). Poloxamer 407 (Lutrol™ F

127) (POL) and poly(butyl methacrylate, [2-dimethyl aminoethyl] methacrylate, methyl methacrylate), 1:2:1 (Eudragit™ EPO) (EUD) were obtained as gifts from BASF (Florham Park NJ, USA) and Röhm (Darmstadt, Germany), respectively. PLGA, 50:50 with inherent viscosity of 0.37 dl/g in hexafluoro isopropanol was purchased from Absorable Polymers International (Pelham AL, USA). BCA monomer (Compont™) was received as gift from Beijing Suncon Medical Adhesive (Beijing, China). Polyvinyl alcohol (PVA) with molecular weight of 67 kDa (86.7–88.7 mol% hydrolysis) and dextran T-70 (D) were supplied by Fluka Chemie (Buchs, Switzerland) and Pharmacia Fine Chemicals (Uppsala, Sweden), respectively. All other chemicals were of analytical grade and used as received.

Methods

Preparation of Chitosan Microparticles

Chitosan solution of 1% w/w in 0.5% w/v acetic acid solution was prepared and subsequently spray dried by using a bench-top spray dryer (Büchi model 190, Büchi Labortechnik, Flawil, Switzerland). The liquid feed was pumped peristaltically and fed through a two-fluid nozzle (0.5 mm internal diameter) where it was atomized into fine droplets. Cooling water was circulated through the jacket around the nozzle throughout the process. The standard processing parameters comprised an atomizing air volumetric flow rate of 750 l/h and the aspirator vacuum of 25 mbar. The inlet drying air temperature and the liquid feed rate were controlled at 120°C and 3 ml/min, respectively. BSA and/or other excipients, including GEL, POL, and EUD, were later incorporated into the chitosan microparticles at 5% and 15% by weight of chitosan, respectively. The materials were separately dissolved in a certain volume of distilled water, subsequently mixed with chitosan solution, in a manner that the final loading of all components in the microparticles was controlled, and spray dried as described above. For cross-linking (C), the spray-dried chitosan or chitosan composite microparticles were dispersed in a few milliliters of absolute ethanol and sonicated with a 3-mm-tip diameter standard probe at an output control of 60 (Vibra Cell model VC 130 PB, Sonics and Materials, Newtown CT, USA) for ~30 s, in order to deaggregate the microparticles. The dispersion was loaded drop-wise by using a micropipette and magnetically stirred (200 rpm, room temperature) in 1% w/v tripolyphosphate solution for 30 min. After the reaction, the particles were filtered, washed three times with distilled water and subsequently vacuum-dried overnight.

Preparation of Poly(Lactic-co-Glycolic Acid) Microparticles

One part of 2.5% w/v BSA solution in distilled water as an aqueous phase and five parts of 10% w/v PLGA solution in dichloromethane as an organic phase were mixed together by means of sonication as described under the 'Preparation of Chitosan Microparticles' section, but at an output control of 100. The mixture was then dispersed into 25 parts of 2% w/v PVA solution by means of sonication with a 6–mm-tip diameter standard probe at an output control of 100 for 30 s, and subsequently transferred to 50 parts of magnetically stirred (200 rpm, room temperature) 0.2% w/v PVA solution. The final mixture was kept stirring for 4–6 h. The particles were separated by centrifugation (Eppendorf model 5810, Eppendorf AG, Hamburg, Germany) at 4000 rpm (1699 × g) for 15 min, washed three times with distilled water and eventually re-dispersed with distilled water to the original volume of dichloromethane.

Preparation of Poly(α-Butyl Cyanoacrylate) Micro-/Nanoparticles

BCA monomer (100 μL) was added drop-wise into 10 ml of either pH 1 or pH 3 hydrochloric acid solution and stirred by using a propeller (200 rpm, room temperature) for 4 h until milky white suspension was obtained. For stabilizer-containing formulations, a required amount of D was first dissolved in the aqueous acidic solution prior to the addition of monomer. After the particles were formed, which took about 1 and 4 h for the polymerization at pH 3 and at pH 1, respectively, pre-dissolved BSA in 0.5 ml of distilled water was added drop-wise into the stirred mixture. The mixture was stirred for another 3–4 h for complete adsorption of protein.

Particle Size Measurement

Particle size and size distribution of chitosan and PLGA microparticles were measured by laser light-scattering method (Mastersizer 2000, Malvern Instrument, Malvern, UK). In case of chitosan microparticles, the particles were first dispersed in a few milliliters of absolute ethanol by means of probe sonication, as previously described under the 'Preparation of Chitosan Microparticles' section, in order to deaggregate the microparticles, and finally loaded into a stirred sample cell, containing deionized water as a measuring medium. Calculation of particle size was made from the intensity of light scattered at different angles, based on Mie's theory (25). The particle size was presented in the volume-weighted mode and the 50% undersize diameter $d(v, 0.5)$ was referred to as the particle diameter. Particle size and size distribution of BCA micro-/nanoparticles were determined by photon correlation spectroscopy (Zetasizer NanoZS, Malvern Instrument, Malvern, UK). Z-average and polydispersity index in the intensity distribution mode were reported as the particle diameter and size distribution, respectively. All the measurements were performed in triplicate.

Zeta Potential Measurement

Chitosan microparticles were dispersed in 1 mM NaCl solution by probe sonication, as described under the 'Preparation of Chitosan Microparticles' section, while other particles were dispersed without sonication. The measurement was carried out on the Zetasizer NanoZS. At least 20 sub-runs were performed at room temperature. The results were reported as zeta potential and zeta deviation.

Particle Morphology

Chitosan microparticles were mounted onto double-faced adhesive tape, which was attached on a sample stub. PLGA microparticles were filtered and vacuum-dried before being mounted onto the sample stub. The samples were coated with gold and viewed under a scanning electron microscope (Jeol model JSM-5410 LV, Tokyo, Japan) at a voltage of 15.0 kV. The photomicrographs were then taken at a magnification of 7500. BCA micro-/nanoparticles were freeze-dried, prepared as described above and viewed under a scanning electron microscope (Jeol model JSM 5600 LV, Tokyo, Japan). The photomicrographs were then taken at a magnification of either 5000 or 10 000.

Surface Analysis

The presence of BSA at or near the particle surface was investigated by X-ray photoelectron spectroscopy (XPS Axis-Ultra, Kratos Analytical, Manchester, UK), using monochromatic Al K_α radiation at 225 W and low-energy electron flooding for charge compensation. All C1s hydrocarbon peak were recalibrated at a binding energy of 284.80 eV to compensate for surface charge effects. The exposure of BSA on the particle surface was calculated by the following equation.

$$\%\ \text{BSA coverage} = \frac{\%\ \text{sulfur exposure on the particle surface} \times 100}{\%\ \text{sulfur exposure on BSA surface}} \quad (1)$$

Protein Content Determination

Chitosan and PLGA microparticles were separately dissolved in 0.5% acetic acid solution and the mixture of 1:1 dimethyl sulfoxide and 0.5% dodecyl sufate in 0.05 N NaOH, respectively. BSA content was determined by using bicinchoninic acid kit for protein determination (Sigma-Aldrich, Singapore). The reaction was run at room temperature for 2 h. Optical density of the sample solution was read at 562 nm on a spectrophotometer (Jasco model V-530, Jasco, Tokyo, Japan). BCA micro-/nanoparticles were separated by centrifugation (Ruijiang model RT-TGL- 16 G, Ruijiang Beijing, China) at 15 000 rpm (20 817 g) for 30 min. The protein content was determined indirectly from the supernatant of the reaction medium, according to Bradford method (26). Briefly, 200 µl of the sample solution were reacted with 2 ml of Bradford working solution (35 mg of Coomassie brilliant blue dissolved in 25 ml 95% ethanol, 50 ml 88% phosphoric acid and 425 ml distilled water) at room temperature for 2 min. Optical density of the sample solution was read at 595 nm on a spectrophotometer (PGeneral model TU-1901, Beijing Purkinje General Instrument, Beijing, China). The actual protein loading and the entrapment efficiency were calculated, according to the following equations. All the experiments were performed in triplicate.

$$\%\ \text{BSA loading} = \frac{\text{Actual weight of BSA} \times 100}{\text{Weight of microparticles}} \quad (2)$$

$$\%\ \text{Entrapment efficiency} = \frac{\text{Actual weight of BSA} \times 100}{\text{Nominal weight of BSA}} \quad (3)$$

In Vitro Release Test

Micro-/nanoparticles (10 mg) were suspended in 1 ml of pH 7.4 phosphate buffered saline (PBS) and then shaken horizontally 120 rpm at 37°C in a shaking incubator (WiseCube® model WIS-20R, Daihan Scientific, Seoul, Korea). At hour 1, 2, 4, day 1, 2, 4, 7, 10 and 14, the supernatant was separated by centrifugation (Eppendorf model 5810, Eppendorf AG, Hamburg, Germany) at 7500 rpm (5974 g) for 10 min for chitosan and PLGA microparticulate samples or as described under the 'Protein Content Determination' section for BCA micro-/nanoparticulate samples. The whole release medium (~1 ml) was collected and assayed for the protein released as described above. New sample tubes were taken at each time point. The experiment was carried out in triplicate.

Protein Integrity

Sodium Dodecyl Sulfate-Polyacrylamide Gel Electrophoresis (SDS-PAGE)

BSA was recovered by dissolving chitosan and PLGA microparticles as described under the 'Protein Content Determination' section. For BCA micro-/nanoparticles, they were shaken with distilled water in the shaking incubator (120 rpm) at room temperature overnight. The supernatant, as the sample solution, was separated as described under the same section. One part of the samples was mixed with one part of reducing sample buffer (5% β-mercaptoethanol in Novex® Tris-Glycine SDS sample buffer; Invitrogen, Calsbad CA, USA) and heated at 95°C for 1 min. The

mixture equivalent to 7.5 μg of BSA was then loaded onto a pH8.8 12% Bis-Tris polyacrylamide gel and subjected to electrophoresis (Bio-Rad model Mini-PROTEAN II, Bio-Rad Laboratories, Hercules CA, USA) in pH 8.3 Novex® Tris-Glycine SDS running buffer (Invitrogen, Calsbad CA, USA) at 80 V for about 2 h. The gel was stained with SimplyBlue™ SafeStain (Invitrogen, Calsbad CA, USA) for 1 h and destained several times with distilled water until the protein bands were visualized.

Circular Dichroism (CD)

BSA was recovered from the micro-/nanoparticles as described under the 'Sodium Dodecyl Sulfate-Polyacrylamide Gel Electrophoresis (SDS-PAGE)' section. The sample solutions were diluted with ultrapure water to obtain about 50 μg/ml of BSA in solution. Ellipticity (θ, mdeg) of the solutions was recorded between 190 and 350 nm on a spectropolarimeter (Jasco model J-715, Jasco, Tokyo, Japan). Molar ellipticity ([θ], deg cm^2 $decimol^{-1}$) was then calculated by the following equation

$$[\theta] = \frac{\theta.\ \mathrm{Mp}}{10\ 000.\ \mathrm{n.\ C'.\ l}} \tag{4}$$

where Mp is molecular weight of BSA (66 430 Da), *n* is number of amino acid residues of BSA (583 residues), C' is concentration of BSA in sample solution (g/ml) and l is path length of cell (0.5 cm). CD spectra were obtained by plotting molar ellipticity against wavelength. The solution of corresponding blank microparticles of each sample was also prepared and run as background.

Cell Viability Study

Mouse DC (CRL-11904) and mouse splenic Mϕ (CRL-2471) were supplied by The American Type Culture Collection. Upon arrival, the cells were subcultured, acoording to the supplier instruction. The passage number about 4–16 was used for the experiments. The cells at the concentration of 5×10^5 cells in 100 μl complete culture medium were separately seeded into each well of 96-well plates and incubated at 37°C with 5% CO_2 in air atmosphere for 24 h. After cells had settled, the particles at varying loading in 100 μl PBS (pH 7.4) were co-incubated with cells for another 24 h at the same condition. Mitochondrial activity of viable cells was measured by Alamar Blue assay (Promega, Madison WI, USA). The reagent (15 μL) was added into each well and incubated at 37°C for 4 h. The percentage of cell viability was calculated by comparing the fluorescence intensity at the excitation wavelength of 540 nm and the emission wavelength of 590 nm (VICTOR^3, Perkin Elmer, USA) of the samples with that of the negative control (cells co-incubated with pH7.4 PBS), which was considered as 100% viability. The corresponding complete culture medium was also run as blank.

In Vitro Cellular Uptake

DC and Mϕ at the concentration of 4×10^6cells in 2 ml complete culture medium were seeded in 6-well plate and incubated at 37°C with 5% CO_2 in air atmosphere until the cell confluency was reached. BSA, chitosan and chitosan composite microparticles, and BCA micro-/nanoparticles were labeled with fluorescein-5-isothiocyanate, isomer I (FITC) (Invitrogen, Calsbad CA, USA), according to the manufacturer's information. For PLGA microparticles, BSA was first labeled by the same procedure and subsequently incorporated into the microparticles. The FITC-labeled micro-/nanoparticles at non-toxic loading were co-incubated with cells for another 4 h at the same condition. The particle uptake was analyzed with a fluorescence-activated cell sorter (FACS) (BD model FACSCalibur, BD Biosciences, San Jose CA, USA), equipped with argon laser. The fluorescence signal was detected with G1 detector for green fluorescence signal at the excitation wavelength of 485 nm and the emission wavelength of 525 nm. The number of fluorescence event, which correlated to the particles internalized within the cells, was counted. The gated cells with fluorescence signal were defined as the positive cells for cellular uptake. The percentage of positive cells relative to the control experiment (cells co-incubated with FITC solution) was then determined and referred to as the uptake capacity, which represents ability of cells to internalize particles. The experiment was counted on at least 20 000 cells.

The uptake process was also observed under a confocal laser scanning electron microscope (CLSM) (Olympus model FV 1000, Olympus, Germany). Glass slips were precoated overnight with 0.01% poly-L-lysine solution (Sigma-Aldrich, Saint Louis MO, USA) and placed in the well plate prior to cell seeding. After incubation with microparticles, the cells were fixed with 3.7% paraformaldehyde in PBS (pH 7.4) and kept in the PBS. The slip was mounted upside-down on a glass slide with glycerin and observed under the microscope with fluorescence detector at the excitation wavelength of 488 nm and the emission wavelength of 520 nm. The photomicrographs were taken at a magnification of 600.

Statistical Analysis

One-way analysis of variance (ANOVA) was performed on BSA loading and *in vitro* release data. Due to unequal variances assumed, the Welch statistic was applied. Data were compared by Dunnett's T3 multiple comparison ($\alpha=0.05$).

RESULTS

Physico-chemical Properties and Morphology of Polymeric Micro-/Nanoparticles

Chitosan and chitosan composite microparticles for cellular delivery of an antigenic protein were prepared by spray drying technique. Physico-chemical characteristics of the microparticles are shown in Table I.

The particle size and uniformity of blank chitosan and chitosan composite microparticles ranged between 3.05–5.45 μm and 0.26–0.53 μm, respectively. The molecular weight and source of chitosan and the incorporation of excipients did not show significant effect on both particle size and uniformity of microparticles. The particles exposed positive surface charge. JCS microparticles exhibited slightly higher average zeta potential than LCS and HCS microparticles. Co-spray drying of GEL along with chitosan induced a remarkable increase in average zeta potential of the resultant microparticles, but not that of POL and EUD. The protein loading and the entrapment efficiency of BSA-loaded chitosan and chitosan composite microparticles ranged between 2.55–4.67% and 50.05–86.72%, respectively. It was noticed that the BSA loading and the entrapment efficiency of GEL LCS and GEL HCS microparticles were a little lower than those of the others ($p > 0.05$). Incorporation of BSA into microparticles increased the particle size, compared to blank microparticles, but with similar size distributions. Meanwhile, the zeta potential of BSA-loaded microparticles was maintained or slightly reduced, except in some cases of the GEL composite microparticles, whose zeta potential was decreased. Nonetheless, their zeta potential was still higher than that of other chitosan and chitosan composite microparticles.

Morphology of chitosan and chitosan composite microparticles are illustrated in Fig. 1.

The blank chitosan microparticles of different molecular weights and/or sources were relatively spherical, with dented surface (Fig. 1a–c). Encapsulation of protein yielded slightly rougher surface than the corresponding blank microparticles (Fig. 1a and d). Inclusion of excipients into chitosan microparticles considerably changed morphology and topography of the particles in different ways. The GEL LCS microparticles had less dented, but more undulate surface than the LCS microparticles (Fig. 1a and e). Addition of POL resulted in the smoother surface of microparticles (Fig. 1g). Incorporation of EUD could eliminate most of dents on the particle surface,

Table I Physico-chemical Properties of Polymeric Micro-/Nanoparticles

	Blank microparticles		BSA-loaded microparticles			
	Size (μm)	Zeta potential (mV)	BSA loading (%)	EE [1] (%)	Size (μm)	Zeta potential (mV)
LCS	3.43 (0.36) [2]	24.97 (3.40) [4]	4.34 [5] (0.08) [4]	86.72	4.51 (0.47) [2]	23.10 (7.26) [4]
GEL LCS	4.12 (0.26)	37.18 (3.54)	2.55 (0.61)	50.05	4.29 (0.57)	29.58 (10.89)
POL LCS	3.11 (0.34)	24.99 (14.81)	3.89 (0.07)	78.33	4.35 (0.46)	23.35 (7.46)
EUD LCS	3.38 (0.53)	27.02 (6.13)	4.50 (0.18)	81.88	4.32 (0.54)	21.95 (6.60)
HCS	3.90 (0.35)	23.70 (4.16)	3.48 (0.74)	72.49	5.96 (0.46)	23.22 (6.72)
GEL HCS	4.47 (0.51)	33.04 (5.59)	2.83 (0.16)	56.89	6.70 (0.29)	33.41 (3.58)
POL HCS	3.40 (0.36)	25.94 (11.09)	3.98 (0.39)	80.12	6.10 (0.45)	25.19 (4.60)
EUD HCS	3.05 (0.38)	25.34 (10.64)	4.37 (0.05)	79.75	3.80 (0.50)	26.09 (7.82)
JCS	5.45 (0.28)	29.12 (3.83)	3.75 (0.03)	75.12	7.18 (0.59)	23.09 (4.19)
GEL JCS	5.33 (0.29)	39.82 (3.99)	3.28 (0.47)	65.98	4.84 (0.42)	29.35 (3.90)
POL JCS	4.36 (0.37)	24.68 (7.04)	4.22 (0.61)	83.79	5.23 (0.40)	22.80 (4.82)
EUD JCS	3.62 (0.46)	28.01 (9.13)	4.67 (0.25)	84.18	5.04 (0.47)	22.13 (4.85)
C LCS	4.29 (0.58)	18.03 (7.11)	3.57	89.03	4.96 (0.52)	16.33 (9.52)
C GEL LCS	14.88 (0.69)	13.07 (5.33)	1.52	64.96	19.80 (3.67)	15.74 (5.59)
C POL LCS	-	-	4.19	100.48	3.13 (0.81)	20.87 (10.72)
C EUD LCS	4.18 (0.55)	27.01 (6.14)	4.08	92.10	3.14 (0.94)	32.57 (11.53)
PLGA	0.94 (0.43)	−1.91 (4.36)	5.33 (0.58)	99.67	6.26 (1.81)	−2.67 (17.90)
BCA 3 D 0	0.46 (0.10) [3]	−28.29 (7.25)	3.58 (1.61)	32.23	0.85 (0.28) [3]	−21.28 (4.65)
BCA 3 D 5	0. 50 (0.19)	−23.55 (4.70)	3.74 (0.26)	19.34	0.90 (0.18)	−18.21 (3.68)
BCA 3 D 10	0.48 (0.03)	−17.56 (5.90)	3.43 (3.22)	20.28	0.93 (0.37)	−16.28 (4.69)
BCA 1 D 5	0.94 (0.53)	−2.21 (8.92)	9.51 (0.01)	97.16	6.34 (0.51)	32.98 (6.52)
BCA 1 D 10	0.80 (0.46)	−1.82 (5.68)	3.88 (0.79)	35.93	0.23 (0.31)	15.52 (10.84)

[1] Entrapment efficiency, [2] Absolute deviation from the median (Uniformity) or [3] polydispersity index, [4] Standard deviation, and [5] $n = 3$

yielding the microparticles with smoother, but matte surface (Fig. 1i). Once BSA was incorporated, the LCS composite microparticles became dented and undulate, with partial distortion (Fig. 1f, h, and j).

Cross-linking of blank LCS microparticles caused a slight increase in particle size and size distribution, but a remarkable decrease in average zeta potential (Table I). In contrast, C GEL LCS microparticles were about 3.6 times larger in size

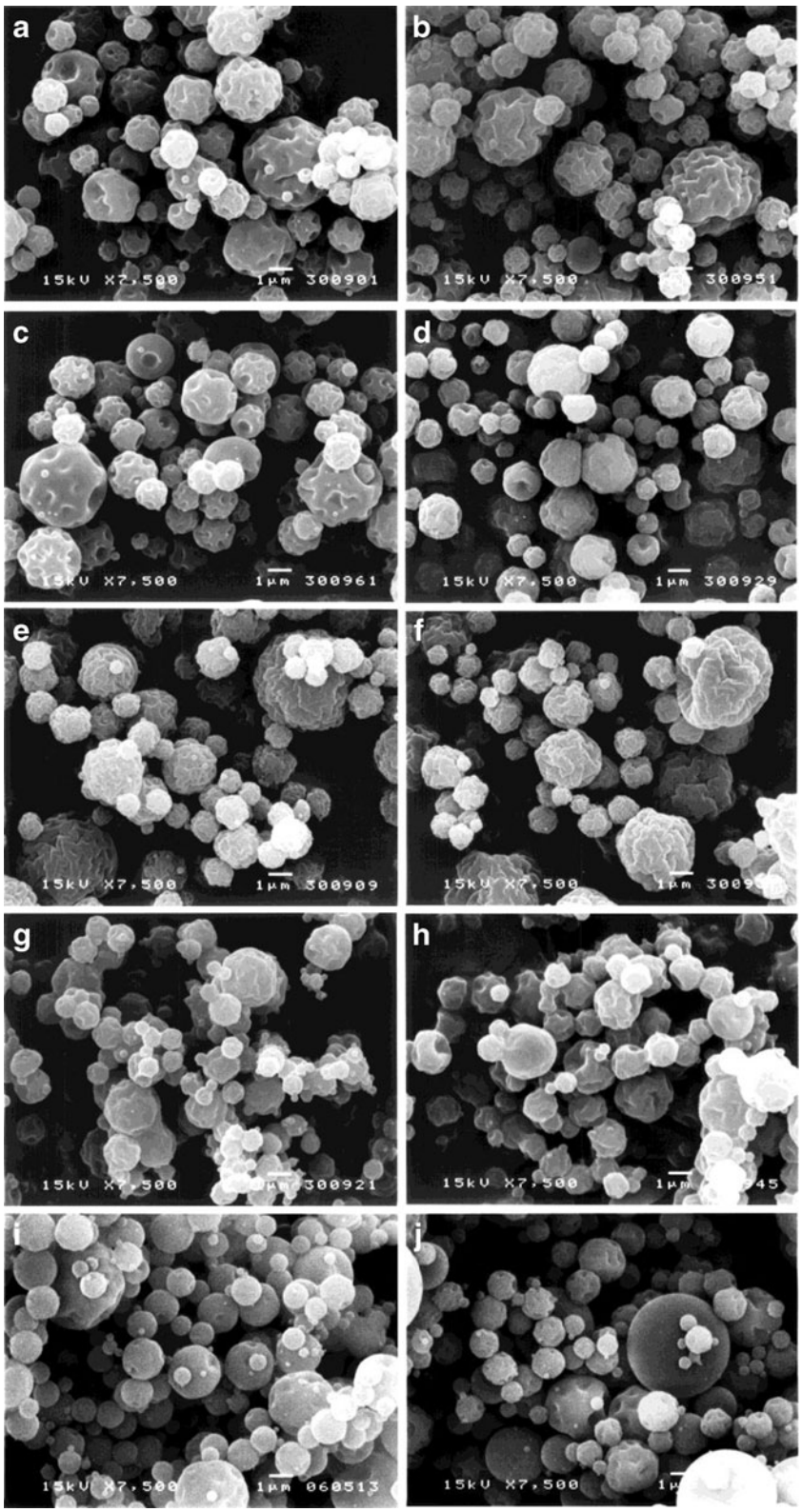

Fig. 1 Scanning electron photomicrographs of chitosan microparticles: (**a**) LCS, (**b**) HCS, (**c**) JCS, (**d**) BSA-loaded LCS, (**e**) GEL LCS, (**f**) BSA-loaded GEL LCS, (**g**) POL LCS, (**h**) BSA-loaded POL LCS, (**i**) EUD LCS, and (**j**) BSA-loaded EUD LCS (The scale bar represents 1 μm).

than the original particles, with a substantial decrease in average zeta potential. The modification process resulted in a slight decrease of protein loading in most cases, except C POL LCS microparticles, whose BSA loading was found to increase slightly from 3.89 to 4.19%. Cross-linking of BSA-loaded chitosan and chitosan composite microparticles yielded similar effects on size and zeta potential to that of the corresponding blank microparticles, except the increased zeta potential of the BSA-loaded C EUD LCS microparticles. The processed BSA-loaded microparticles had a very smooth surface (Fig. 2), although some and many distorted particles were observed in cases of C LCS and C GEL LCS microparticles, respectively (Fig. 2a and b).

PLGA and BCA micro-/nanoparticles were prepared by double-emulsion solvent-evaporation and anionic polymerization technique, respectively. The physico-chemical properties and morphology of particles are presented in Table I and Fig. 3, respectively.

Blank PLGA microparticles were relatively small, compared with the blank chitosan and chitosan composite microparticles. The particles were fairly neutral, with slightly-negative zeta potential. BSA loading and entrapment efficiency of the microparticles were satisfactorily high. Upon protein encapsulation, the microparticles became much larger both in size and size distribution and comparable in size to the BSA-loaded chitosan and chitosan composite microparticles. In contrast, the zeta potential was maintained. Both blank and BSA-loaded PLGA microparticles were perfectly spherical, with very smooth surface (Fig. 3a and b). It was conceivable that encapsulation of protein resulted only in larger particle size, without any effect on the surface topography of particles.

BCA micro-/nanoparticles were prepared at two pH levels (1 and 3) and various D concentrations (0, 5 and 10% w/v), which were indicated in the nomenclature of particles. Polymerization at pH 3 yielded the comparable-sized nanoparticles, with narrow size distribution, independent of D concentration. These nanoparticles exposed negative surface charge. The zeta potential decreased, as D concentration was increased. In contrast, stabilizer played a very important role on the particle preparation at pH 1. Without D, the agglomerated white material floating on the surface of polymerization medium was obtained. The nanoparticles could be collected only when D was added. These nanoparticles were larger than those prepared at pH 3. The particle size was reduced as the concentration of D was increased. Surprisingly, the nanoparticles were relatively neutral, with slight negative zeta potential.

The protein loading of nanoparticles polymerized at pH 3, but different D concentrations, was comparable to each other. Meanwhile, the entrapment efficiency was reduced, once D was incorporated. Both properties were not affected by the varied D concentrations. The BSA-loaded BCA micro-/nanoparticles were approximately doubled in size, compared to the unloaded particles, along with slight reduction of zeta potential. Increasing D concentration did not have much effect on both size and zeta potential of the BSA-loaded particles. In case of polymerization at pH 1, protein loading and entrapment efficiency of the particles, stabilized with 5% w/v D, were surprisingly high ($p<0.05$), whereas those of the particles stabilized with higher D concentration were reduced to the comparable extent to those prepared at pH 3 ($p>0.05$). Particle size of BSA-loaded BCA 1 D 5 microparticles, which was polymerized at pH 1 with 5% w/v D as the stabilizer, was increased to the same size range of BSA-loaded chitosan and PLGA microparticles. However, when the D concentration was increased to 10%

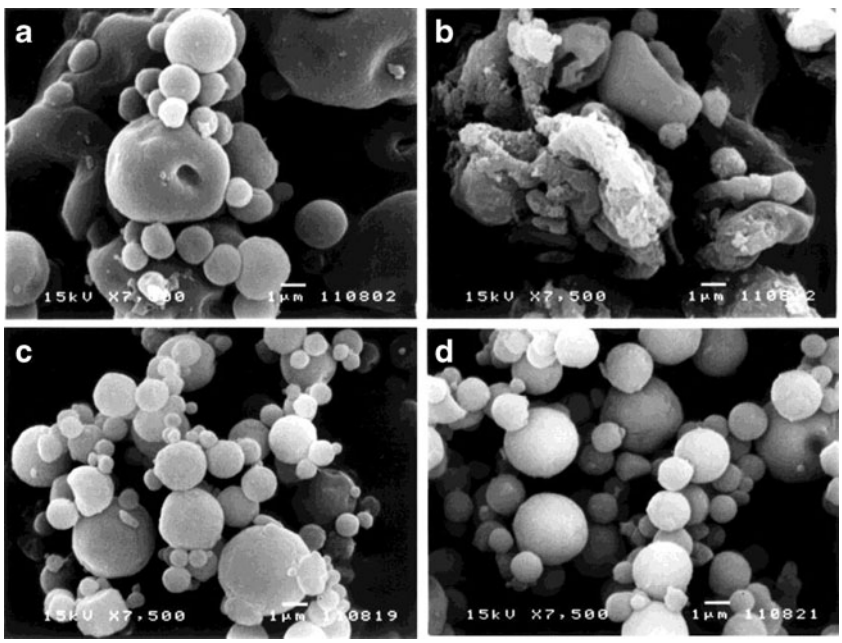

Fig. 2 Scanning electron photomicrographs of cross-linked BSA-loaded chitosan microparticles: (**a**) LCS, (**b**) GEL LCS, (**c**) POL LCS, and (**d**) EUD LCS (The scale bar represents 1 μm).

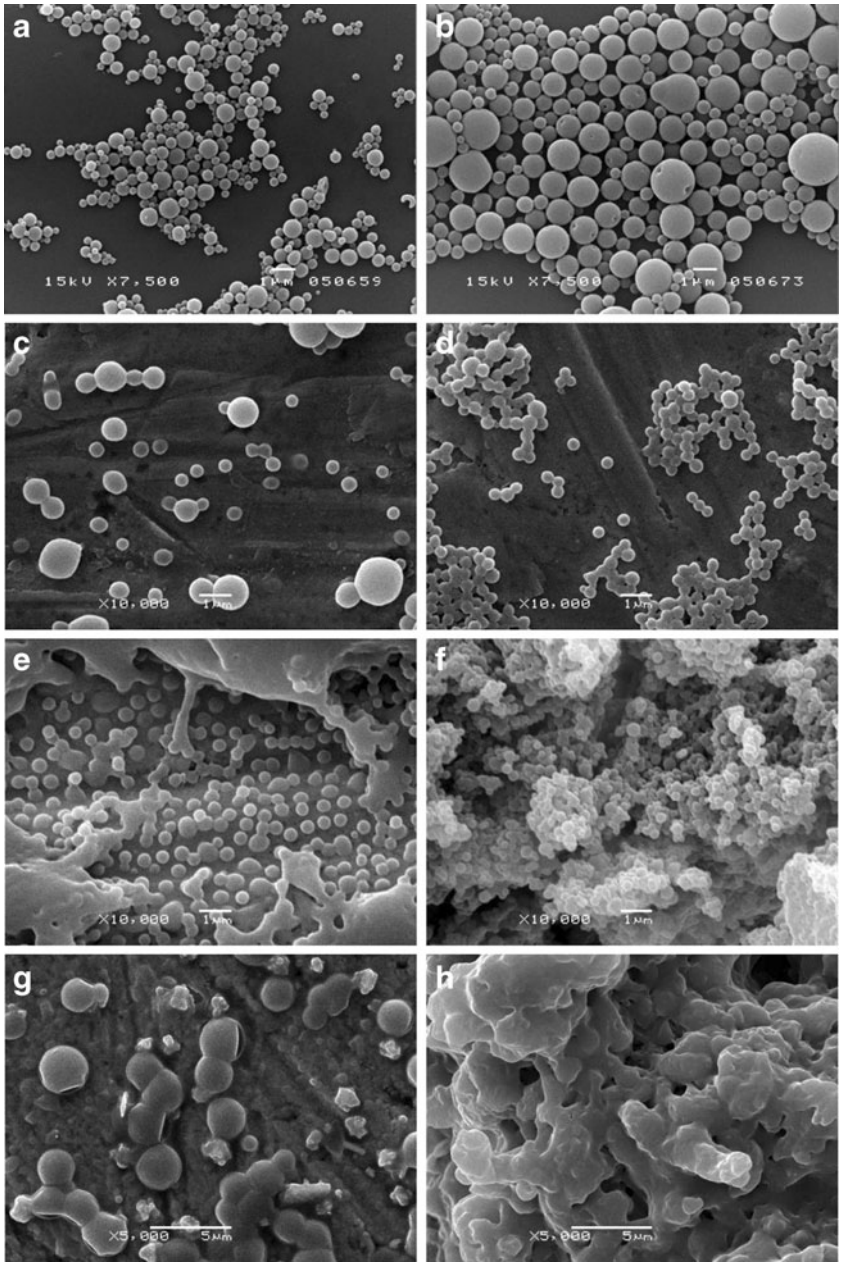

Fig. 3 Scanning electron photomicrographs of PLGA microparticles and BCA micro-/nanoparticles: (**a**) PLGA, (**b**) BSA-loaded PLGA, (**c**) BCA 3 D 0, (**d**) BSA-loaded BCA 3 D 0, (**e**) BCA 3 D 10, (**f**) BSA-loaded BCA 3 D 10, (**g**) BCA 1 D 10, and (**h**) BSA-loaded BCA 1 D 10 (The scale bar represents 1 μm).

w/v, the size of BSA-loaded particles became smaller than the corresponding blank microparticles. Surprisingly, the zeta potential of nanoparticles became positive after the adsorption of protein. It decreased, as the D concentration was increased. It was noted that the nanoparticles prepared at this pH were widely distributed in their particle size.

Polymerization at pH3 without stabilizer yielded the smooth spherical nanoparticles (Fig. 3c). When 10% w/v D was added into the polymerization medium, the small and more uniform-sized nanoparticles were obtained (Fig. 3e). In contrast, fabrication of nanoparticles at pH1 in the presence of 10% w/v D yielded the relatively large and partly-deformed particles (Fig. 3g). Upon BSA loading, an agglomeration of nanoparticles was observed (Fig. 3d). The effect was more pronounced, as the loading was carried out with D and/or at lower pH (Fig. 3f and g).

Type and amount of elements exposed on the surface of micro-/nanoparticles were investigated by XPS. The results are shown in Table II.

Characteristic exposure of nitrogen, attributed to the amino groups on polymer backbone, was detected on the surface of chitosan microparticles. Co-spray drying of LCS with GEL, POL and EUD resulted in the increased, decreased, and maintained proportion of nitrogen exposure, respectively. Upon incorporation of BSA, the BSA coverage on the particle surface, indicated by the exposure of sulfur, was detected. It was reduced, when the excipients were incorporated, and totally undetectable in case of the POL

LCS microparticles. Surface composition of blank and BSA-loaded PLGA microparticles was alike. No exposure of sulfur was detected on the surface of protein-loaded particles. However, it was noticed that a significant amount of silicon was found on the surface of microparticles. Source of the element was actually unknown, since there was no evidence in both PLGA and the solvents used for particle preparation. BCA micro-/nanoparticles were freeze-dried, prior to XPS study. Unfortunately, the blank BCA micro-/nanoparticles could not be dried properly and hence the surface composition analysis could not be performed. For BSA-loaded BCA micro-/nanoparticles, deposition of BSA on the particle surface was detected only on the surface of those polymerized at pH3 with 10% w/v D.

In Vitro Release Test

The release of BSA from micro-/nanoparticles was performed *in vitro* in PBS (pH 7.4) at 37°C. The profiles are illustrated in Fig. 4.

While the LCS microparticles gradually released the protein throughout the time course of release study, the higher molecular weight of HCS and JCS microparticles burstly released BSA within a few hours (37.87% in 4 h and 60.46% in 1 h, respectively). The maximum release was reached at about 40% and 80% within the first and the second day of the test, for HCS and JCS microparticles, respectively (Fig. 4a). Modification of LCS microparticles, either by co-spray drying with the excipients or cross-linking with the phosphate anions, changed the release behavior of BSA substantially. The GEL LCS microparticles released a higher amount of BSA and faster than the LCS microparticles. Meanwhile, the POL LCS and the EUD LCS microparticles burstly released BSA within a few hours (53.77% in 4 h and 54.84% in 1 h, respectively). The stable phase of protein release was obtained within a day and a few days for the POL LCS and the EUD LCS microparticles, respectively. It was noticed that the EUD LCS microparticles yielded a little higher amount of BSA released than the POL LCS microparticles ($p > 0.05$). In contrast, only 26.12% of protein was gradually released from C LCS microparticles within the time course of release test.

PLGA microparticles released the protein most slowly. Only about 3% of encapsulated BSA was released within 4 weeks (Fig. 4b). Generally, the BSA-adsorbed BCA micro-/nanoparticles prepared at pH 3 released the protein in a faster manner than those prepared at lower pH (Fig. 4b). Without stabilizer, they gave a burst release of protein and reached the maximum release within two days. Incorporation of D caused a slower release, along with the higher amount of liberated BSA at the maximum release. For the micro-/nanoparticles produced at pH 1, the protein was released at the comparable rate to each other, although it was later released more from the particles stabilized with 10% w/v D.

Integrity of Encapsulated BSA

The integrity of encapsulated protein was confirmed by SDS-PAGE. All bands of BSA, recovered from chitosan (Fig. 5a), chitosan composite (Fig. 5b) and PLGA (Fig. 5c) microparticles, moved in a comparable distance to BSA in the molecular weight standards and the unprocessed BSA. No band was observed in either higher or lower molecular weight region. Smear appeared on the lanes of BSA-loaded chitosan and chitosan composite microparticles was believed to be staining of chitosan and/or the excipients, since it was also evident on the lanes of corresponding blank microparticles. However, the protein bands of BCA micro-/nanoparticles could not be visualized on the electrophoretic gel (Fig. 5c).

Additionally, the structural conformation of entrapped BSA was investigated by CD. The CD spectra of BSA,

Table II Percentage of Elements Exposed and BSA Coverage on the Particle Surface

Particles	Elements on blank particles (%)				Elements on BSA-loaded particles (%)					BSA coverage (%)
	C	O	N	Other	C	O	N	S	Other	
BSA					65.56	18.97	14.57	0.62	*u.d.*	100.00
LCS	67.47	25.81	6.72	*u.d.*	69.06	16.86	13.70	0.38	*u.d.*	61.29
GEL LCS	65.89	18.09	16.02	*u.d.*	66.90	18.22	14.59	0.29	*u.d.*	46.77
POL LCS	74.40	24.71	0.89	*u.d.*	71.36	26.88	1.76	*u.d.*	*u.d.*	*u.d.*
EUD LCS	75.35	18.62	6.03	*u.d.*	77.34	18.77	3.76	0.13	*u.d.*	20.97
PLGA	53.79	24.72	*u.d.*	Si, 21.48	55.07	24.94	*u.d.*	*u.d.*	Si, 19.99	*u.d.*
BCA 3 D 0					74.98	16.42	8.60	*u.d.*	*u.d.*	*u.d.*
BCA 3 D 10					73.09	17.15	9.62	0.14	*u.d.*	22.58
BCA 1 D 10					72.86	18.17	8.97	*u.d.*	*u.d.*	*u.d.*

u.d. = undetectable

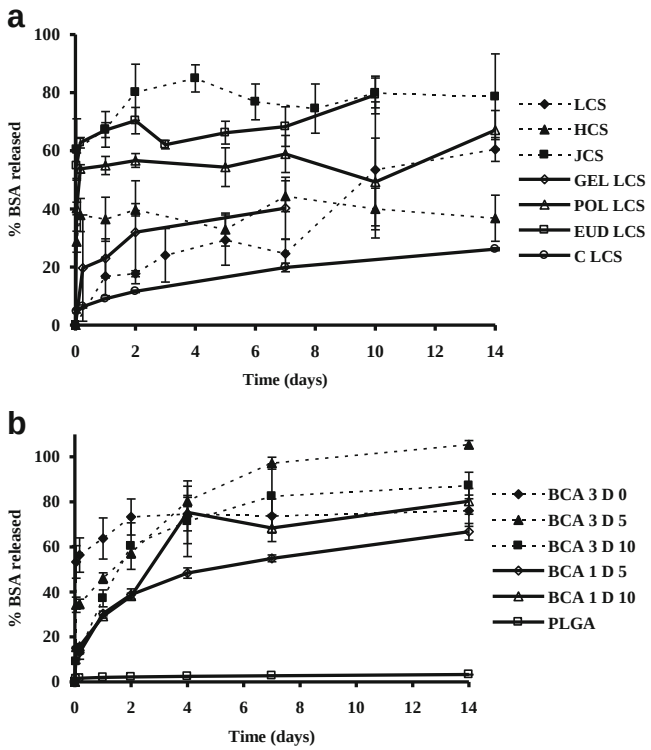

Fig. 4 *In vitro* BSA released from (**a**) chitosan microparticles and (**b**) PLGA microparticles and BCA micro-/nanoparticles, as a function of time (The values represent mean of three samples).

recovered from the LCS and the HCS microparticles, were completely identical, although they exhibited lower molar ellipticity in some degrees than that of the unprocessed BSA (Fig. 6a). In contrast, JCS was able to absorb the polarized UV light to some extent as illustrated in Fig. 6a. The CD spectrum of BSA recovered from the JCS microparticles showed both lower molar ellipticity and different shape, compared to that of the unprocessed BSA (Fig. 6a).

Incorporation of GEL into the LCS microparticles obviously caused lower molar ellipticity and different shape of the BSA CD spectrum, compared with the untreated BSA (Fig. 6b). In contrast, addition of POL and EUD did not change the CD spectra of entrapped BSA significantly (Fig. 6b). In case of PLGA microparticles, the proper CD spectrum of the encapsulated protein could not be obtained (Fig. 6b). Furthermore, a substantially low molar ellipticity of BSA extracted from BCA micro-/nanoparticles was also observed (Fig. 6b).

Cell Viability Study

The polymeric micro-/nanoparticles were subject to the cell viability study with two antigen presenting cells. The effect of particle loading on viability of DC and Mϕ was depicted in Figs. 7 and 8, respectively. Typically, the percentage of cell viability increased as the particle loading was decreased. Although the DC viability profiles of LCS and HCS microparticles were comparable to each other (Fig. 7a), the 100% cell viability was obtained at the particle loading of 1.02 and 0.53 mg/ml, respectively. The viability profile of JCS microparticles was achieved at lower particle loading (Fig. 7a). The 100% DC viability was expected to be gained at the particle loading of less than 0.1 mg/ml. The LC_{50} was calculated to be 8.79, 5.78, and 1.92 mg/ml for LCS, HCS, and JCS microparticles, respectively.

Incorporation of GEL and POL into the LCS microparticles did not change the DC viability profile significantly (Fig. 7a). The 100% cell viability was obtained at particle loading of 0.51 and 1.01 mg/ml for GEL LCS and POL LCS microparticles, respectively. In contrast, incorporation of EUD shifted the DC viability profile to the left (Fig. 7a). Consequently, the 100% DC viability could not be obtained within the investigated range of particle loading. The LC_{50} was achieved at the particle loading of 1.77, 4.97 and 0.15 mg/ml for GEL LCS, POL LCS and EUD LCS microparticles, respectively. In addition, cross-linking of LCS microparticles resulted in similar effect to the EUD LCS microparticles, but in a lesser extent. The LC_{50} was estimated to be 1.16 mg/ml.

The 100% DC viability and the LC_{50} of PLGA microparticles were obtained at the particle loading as high as 4.93 and 16.78 mg/ml, respectively (Fig. 7b). BCA micro-/nanoparticles showed different viability profiles on the far left (Fig. 7b), compared with other microparticles. The nanoparticles, polymerized at pH 3, yielded the 100% cell viability and the LC_{50} at particle loading of 0.02 and 0.10 mg/ml, respectively. Upon D incorporation, the viability profiles were obtained at higher particle loading. Stabilization with 5 and 10% w/v D yielded the 100% DC viability at higher particle loading of 0.05 and 0.11 mg/ml, respectively, and the LC_{50} at higher particle loading of 0.31 and 0.54 mg/ml, respectively. In contrast, the micro-/nanoparticles, prepared at pH 1, gave the 100% DC viability and the LC_{50} at much lower particle loading of 0.005 and 0.02 mg/ml, respectively.

In the study with Mϕ, the cell viability profiles were generally obtained at lower particle loading than those obtained with DC (Fig. 8a). When the LCS microparticles were incubated with Mϕ, the 100% cell viability and the LC_{50} were achieved at particle loading of 0.12 and 2.32 mg/ml, respectively. In contrast to the test with DC, the HCS microparticles yielded the Mϕ viability profile at lower particle loading than both LCS and JCS microparticles (Fig. 8a). For GEL LCS microparticles, the 100% cell viability and the LC_{50} were achieved at particle loading of 0.03 and 1.28 mg/ml, respectively. At all investigated particle concentrations of lower than 0.25 mg/ml, the POL LCS microparticles could give the 100% Mϕ viability, while the EUD LCS microparticles could not. The C LCS microparticles surprisingly produced a comparable cell viability profile to that of the GEL LCS

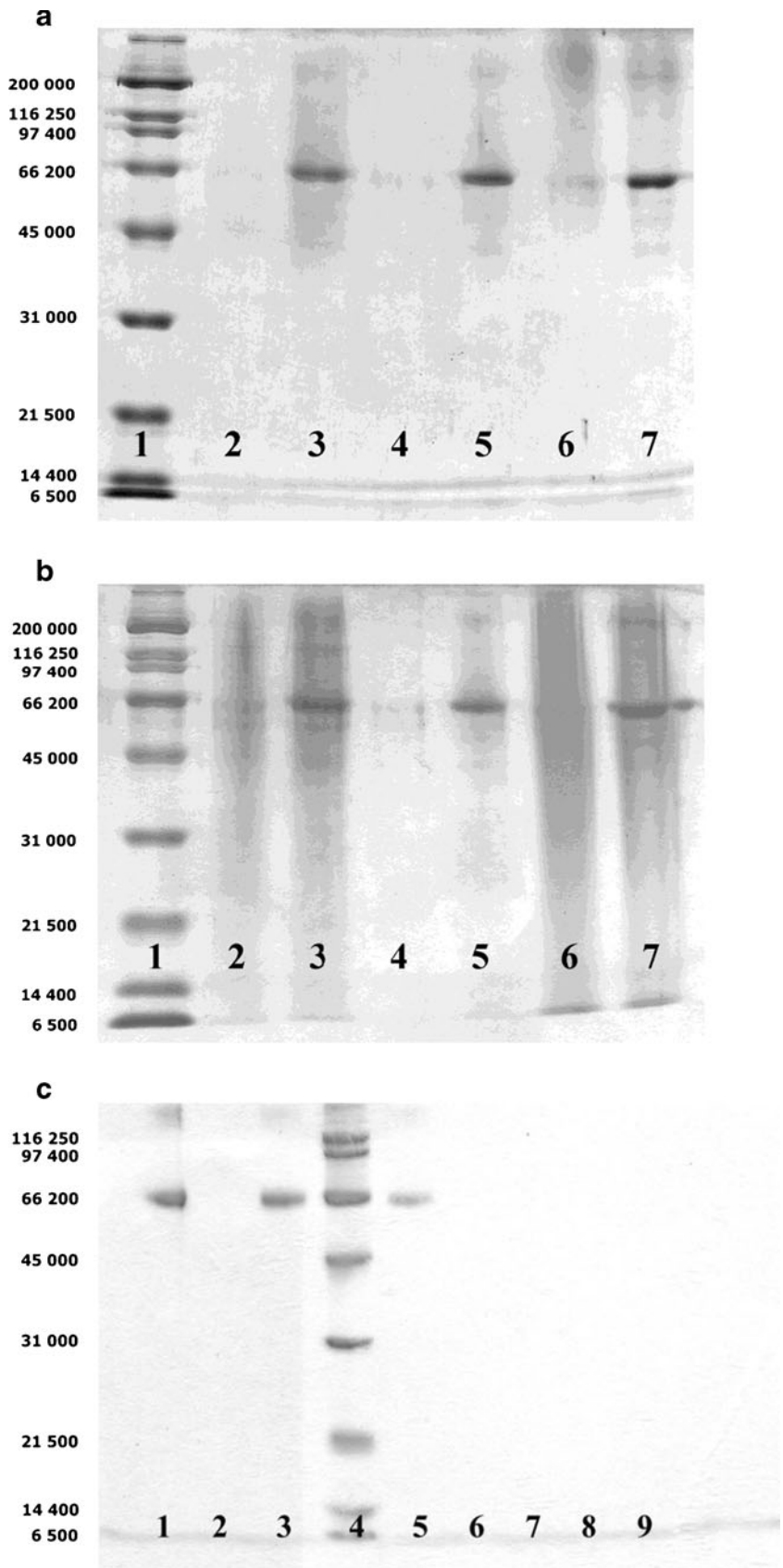

Fig. 5 SDS-PAGE of (**a**) Lane 1: molecular weight standards, broad range (Bio-Rad Laboratories, Hercules CA, USA), Lane 2: LCS, Lane 3: BSA-loaded LCS, Lane 4: HCS, Lane 5: BSA-loaded HCS, Lane 6: JCS, Lane 7: BSA-loaded JCS, (**b**) Lane 1: molecular weight standards, broad range, Lane 2: GEL LCS, Lane 3: BSA-loaded GEL LCS, Lane 4: POL LCS, Lane 5: BSA-loaded POL LCS, Lane 6: EUD LCS, Lane 7: BSA-loaded EUD LCS, and (**c**) Lane 1: unprocessed BSA, Lane 2 PLGA, Lane 3: BSA-loaded PLGA, Lane 4: molecular weight standards, broad range, Lane 5: 1.5 μg unprocessed BSA, Lane 6: BSA-loaded BCA 3 D 0, Lane 7: BSA-loaded BCA 3 D 5, Lane 8: BSA-loaded BCA 3 D 10, and Lane 9: BSA-loaded BCA 1 D 10.

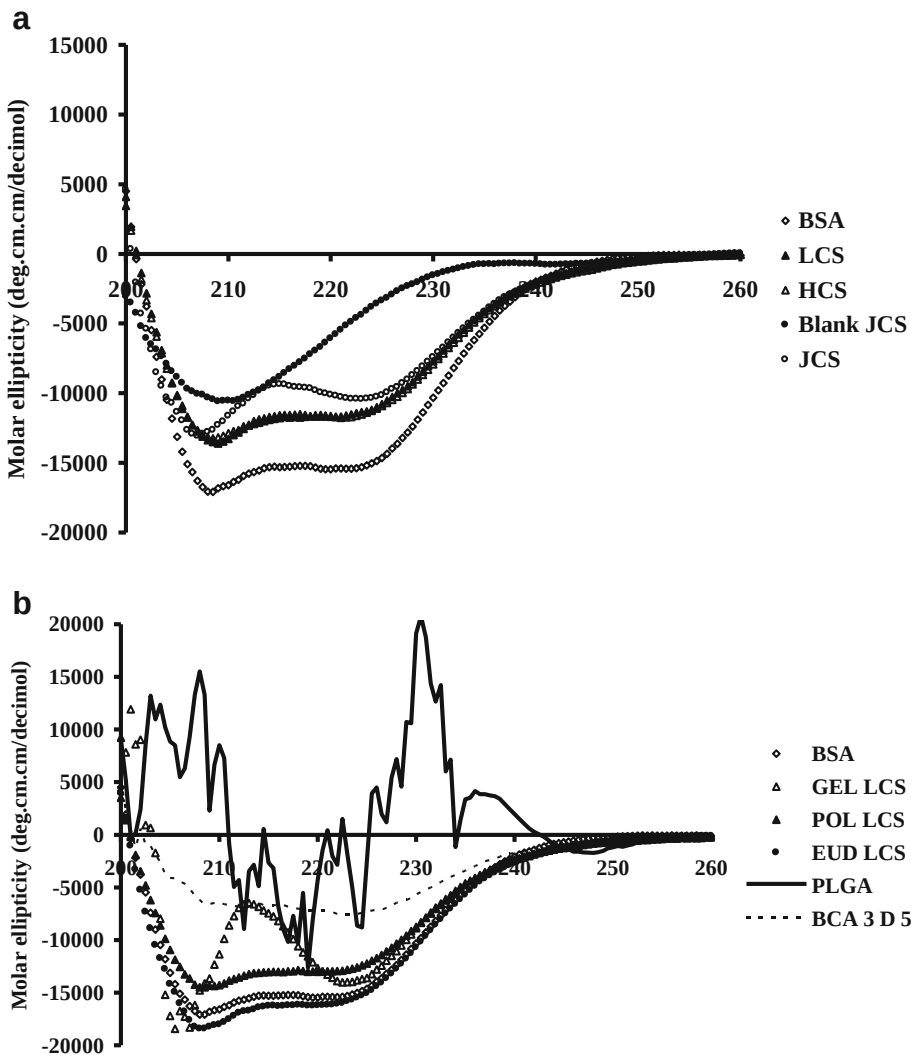

Fig. 6 CD spectra of BSA recovered from BSA-loaded polymeric micro-/nanoparticles: (**a**) chitosan microparticles, and (**b**) chitosan composite microparticles, PLGA microparticles, and BCA micro-/nanoparticles.

microparticles (Fig. 8a and b). The 100% Mϕ viability and the LC_{50} were obtained at the particle loading of 0.03 and 0.54 mg/ml, respectively.

PLGA microparticles yielded the 100% Mϕ viability at all investigated particle loading of lower than 0.25 mg/ml (Fig. 8b). The BCA micro-/nanoparticles, prepared at pH 3, gave the comparable Mϕ viability profiles to one another, independent of D concentration (Fig. 8b). Polymerization at pH1 resulted in the cell viability profile at much lower particle loading (Fig. 8b). Unfortunately, the 100% cell viability could not be obtained within the investigated range of particle loading for all BCA micro-/nanoparitlcles.

In Vitro Cellular Uptake

The prospective micro-/nanoparticles, which were found cytocompatible in the previous section, were labeled with FITC and subsequently incubated with the antigen presenting cells at non-toxic particle loading. The cellular uptake was detected by FACS analysis. The FACS histograms and the uptake capacity are shown in Figs. 9 and 10 for DC and Mϕ, respectively.

The cellular uptake of soluble LCS was not significantly different from the control DC (Fig. 9a and b). More efficient uptake was observed, when DC was co-incubated with the soluble BSA (Fig. 9c). The uptake capacity of DC was further increased to 49.00%, as the microparticulate LCS was tested (Fig. 9d). However, the uptake of HCS and JCS microparticles (Fig. 9e and f) was lower than that of the LCS microparticles. Modification of the LCS microparticles with GEL yielded the comparable uptake capacity to that of the LCS microparticles (Fig. 9d and g). The most efficient uptake of 74.45% was obtained from the POL LCS microparticles (Fig. 9h). The internalization of PLGA and BCA micro-/nanoparticles (Fig. 9i–k) was lower than those of the LCS and the LCS

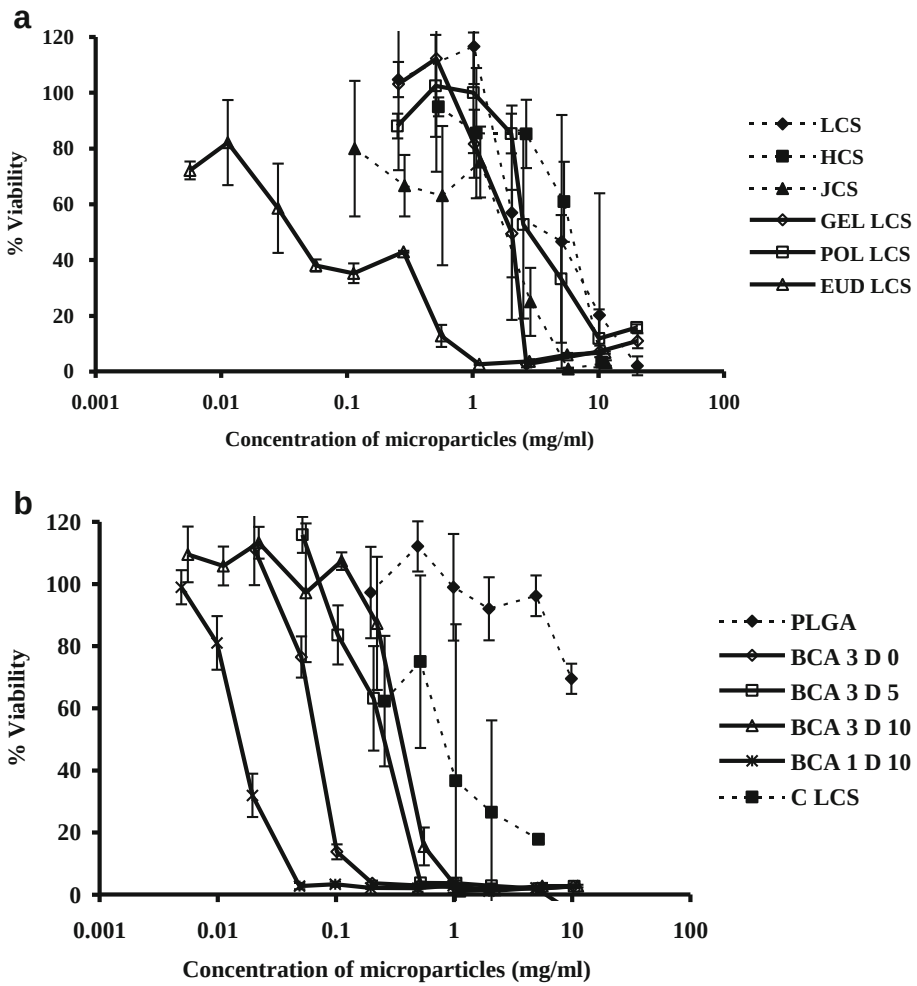

Fig. 7 Percentage of cell viability, relative to control cells, after co-incubation of DC with polymeric micro-/nanoparticles: (**a**) chitosan microparticles and (**b**) PLGA microparticles and BCA micro-/nanoparticles, as a function of micro-/nanoparticle loading (The values represent mean of three samples).

composite microparticles, but comparable to that of the HCS microparticles.

Mϕ could not internalize the soluble form of both LCS and BSA efficiently (Fig. 10b and c), compared with the control Mϕ (Fig. 10a). In addition, the cells were about 6 times less efficient in uptake of the soluble BSA than DC (Figs. 9c and 10c). The uptake capacity of Mϕ was dramatically increased to 80.65%, when the cells were co-incubated with the LCS microparticles (Fig. 10d). This was substantially higher than the uptake by DC (Fig. 9d). While the uptake of HCS microparticles (Fig. 10e) was comparable to that of the LCS microparticles, the uptake of JCS microparticles was surprisingly low (Fig. 10f). Modification of the LCS microparticles with GEL resulted in a little reduction of cellular uptake, whereas the modification with POL did not affect the uptake capacity significantly (Fig. 10g and h), compared with the uptake of LCS microparticles. The uptake of PLGA and BCA micro-/nanoparticles was lower than that of the chitosan and the chitosan composite microparticles. In general, it was conceivable that Mϕ could internalize all the investigated microparticles more efficiently than DC.

In addition, the particle uptake of DC and Mϕ was evidenced under the CLSM. The examples of LCS and GEL LCS uptake were illustrated in Fig. 11. The results corresponded well with those obtained from the FACS analysis.

DISCUSSION

The biocompatible and/or biodegradable micro-/nanoparticles intended for cellular delivery of an antigenic protein were prepared. Chitosan has been generally regarded as a biocompatible and biodegradable material (19). Its utilization for delivery of protein therapeutics and antigens was extensively reviewed (27). In this study, the aqueous acidic solution of chitosan was spray dried under controlled conditions. The microparticles of different molecular weights and sources did not differ from one another, in terms of physico-chemical characteristics and morphology, similarly to results obtained in a previous study (20). Properties of chitosan microparticles were modified by co-spray drying with the acceptable pharmaceutical excipients. GEL has been widely used as a stabilizer in

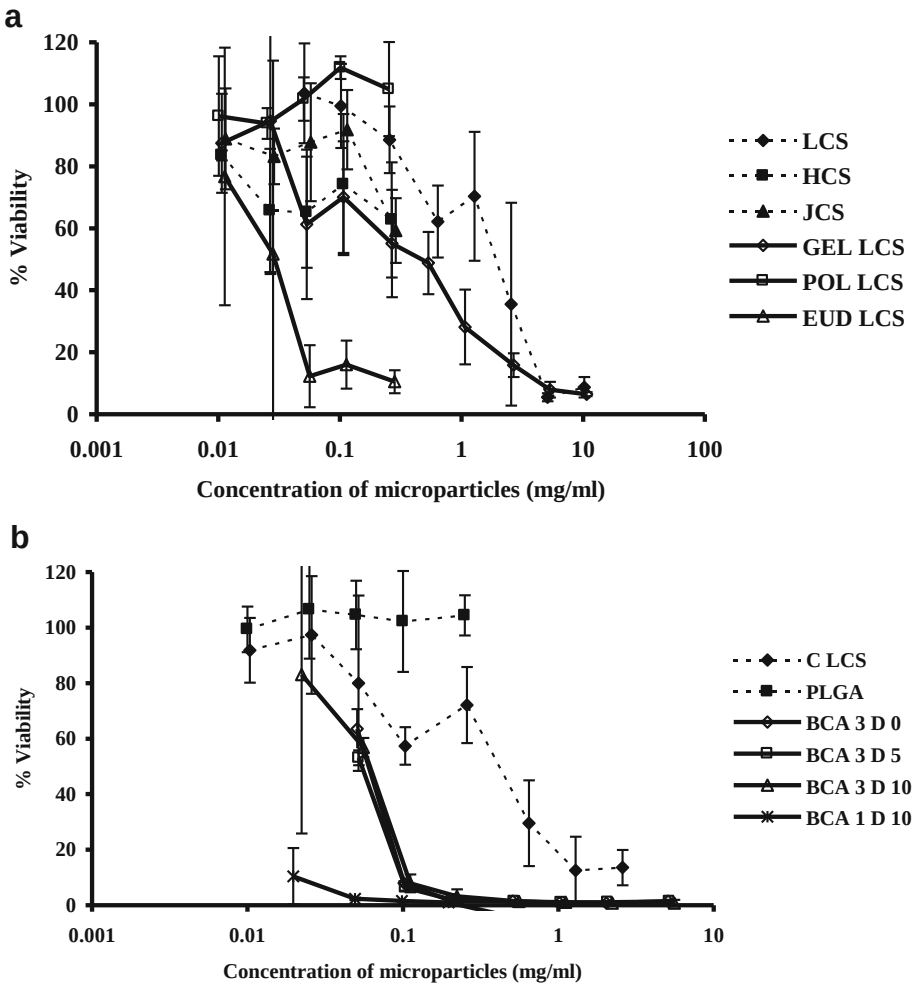

Fig. 8 Percentage of cell viability, relative to control cells, after co-incubation of Mφ with polymeric micro-/nanoparticles: (**a**) chitosan microparticles and (**b**) PLGA microparticles and BCA micro-/nanoparticles, as a function of micro-/nanoparticle loading (The values represent mean of three samples).

several protein and vaccine formulations (28–32). When proteins are partially disrupted or produce molten globule-like states, they tend to readily associate. GEL likely binds to the intermediate states of protein, thereby leading to the stabilizing effects on the onset of the aggregation (33). Interestingly, it also conferred a higher positive zeta potential to the chitosan microparticles, attributed to large numbers of cationic charged residues, including histidine, lysine, hydroxylysine, and arginine (34) . This was also confirmed by the increased proportion of nitrogen exposure found in the XPS study.

Upon atomization, proteins are prone to accumulate at the air-liquid interface of the droplets. Exposure to the large interface during spraying frequently causes the adsorbed proteins to unfold, expose hydrophobic regions and undergo denaturation (35). Incorporation of a surfactant into the formulations prepared for spray drying can enhance protein stability by reducing protein-interface interactions (36). POL is a non-ionic surfactant that has been used in pharmaceutical formulations for its protein stabilizing properties (16,18). In addition, its combination with chitosan markedly enhanced the immune response to intranasal antigen administration (37,38). This would be beneficial for further application of the system as a vaccine carrier. The decreased proportion of nitrogen exposure observed in the XPS study indicated the accumulation of POL at the particle surface. Nevertheless, it did not influence the zeta potential of POL LCS microparticles, likely contributed to non-ionic nature of the surfactant. However, it obviously affected morphology and topography of the particles. Due to its low melting point at about 56°C (39), POL partly melted at the drying temperature and bound the adjacent microparticles together upon later solidification.

EUD possesses the pH-dependent membrane-disruptive property (40). Following phagocytosis, EUD-containing microparticles could enhance delivery of encapsulated protein into an intracellular compartment instantaneously in response to a low pH (5 to 6.5) of the phagosome (41). For vaccination, the process markedly enhances antigen presentation, T cell stimulation, and the resulting cytotoxic T lymphocyte response (42). In this study, EUD seemed to distribute evenly in the microparticulate LCS matrix since its incorporation did not change the proportion of nitrogen exposure on the particle surface and the zeta potential of microparticles. In addition, a good appearance of microparticles was also obtained.

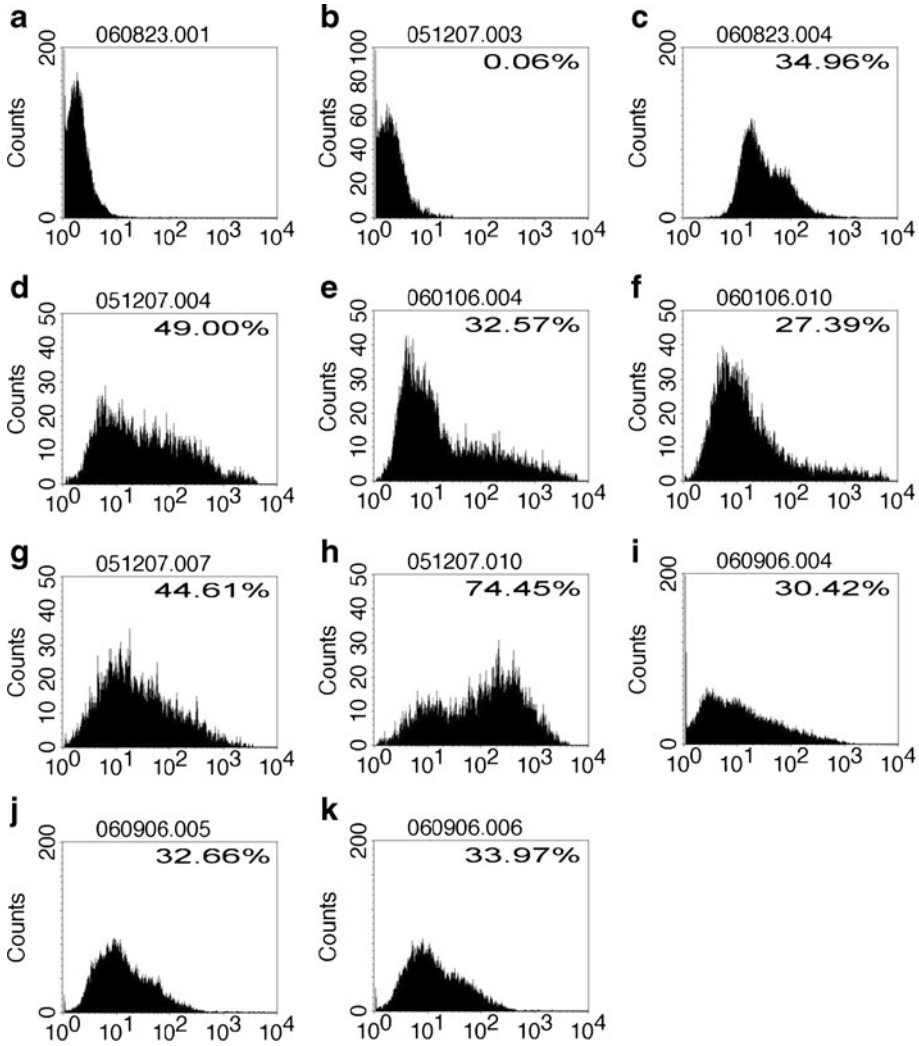

Fig. 9 FACS histograms of (**a**) control DC and gated cells after co-incubation of DC with (**b**) soluble chitosan, (**c**) soluble BSA, and BSA-loaded polymeric micro-/nanoparticles: (**d**) LCS, (**e**) HCS, (**f**) JCS, (**g**) GEL LCS, (**h**) POL LCS, (**i**) PLGA, (**j**) BCA 3 D 5, and (**k**) BCA 3 D 10.

Ionic cross-linking of preformed chitosan and chitosan composite microparticles with tripolyphosphate anions resulted in a considerable change of both physico-chemical properties and morphology of the particles. Due to weak acidic characteristics, the mean charge number and charge density of tripolyphosphate increased as pH of the solution was increased. In contrast, the ionization of amino groups of chitosan, as a weak polybase, decreased as the pH was increased. Therefore, the optimal electrostatic interaction between tripolyphosphate and chitosan would exist only at a certain pH range (43). In this study, the cross-linking was performed at pH 5, where an optimal reaction was obtained (44). During the process, the ionic inter-molecular linkages between the positively charged amino groups of chitosan and the negatively charged groups of tripolyphosphate are formed (38,45), resulting in neutralization of zeta potential. The cationic charged groups of GEL in the composite microparticles likely participated in the cross-linking reaction with tripolyphosphate anions in a large extent (27). As a consequence, a significant reduction of zeta potential and agglomeration of several deformed microparticles were obtained. POL and EUD accumulated at the particle surface might impede the cross-linking process between chitosan and tripolyphosphate in some degrees, according to a slightly-reduced zeta potential of microparticles. Additionally, smoother spherical microparticles were received.

Incorporation of BSA into the microparticles usually resulted in slightly larger particles (20,38,45). Analysis of particle surface composition confirmed the accumulation of BSA at the particle surface. At neutral pH, BSA (pI 4.7 to 4.9) (46,47) likely exposes negative charges. Consequently, the zeta potential of microparticles was reduced. The excipients were found to compete with BSA for accumulation at the particle surface. Especially, POL totally replaced surface BSA, since no signal of sulfur exposure was detected on the particle surface. Similar result was obtained in a previous study (36).

Dispersing chitosan microparticles into the release medium, the burst release of BSA accumulated at the particle surface usually occurred, followed by the slow and continuous release of the protein encapsulated in the inner matrix of microparticles (45). In case of HCS microparticles, only the

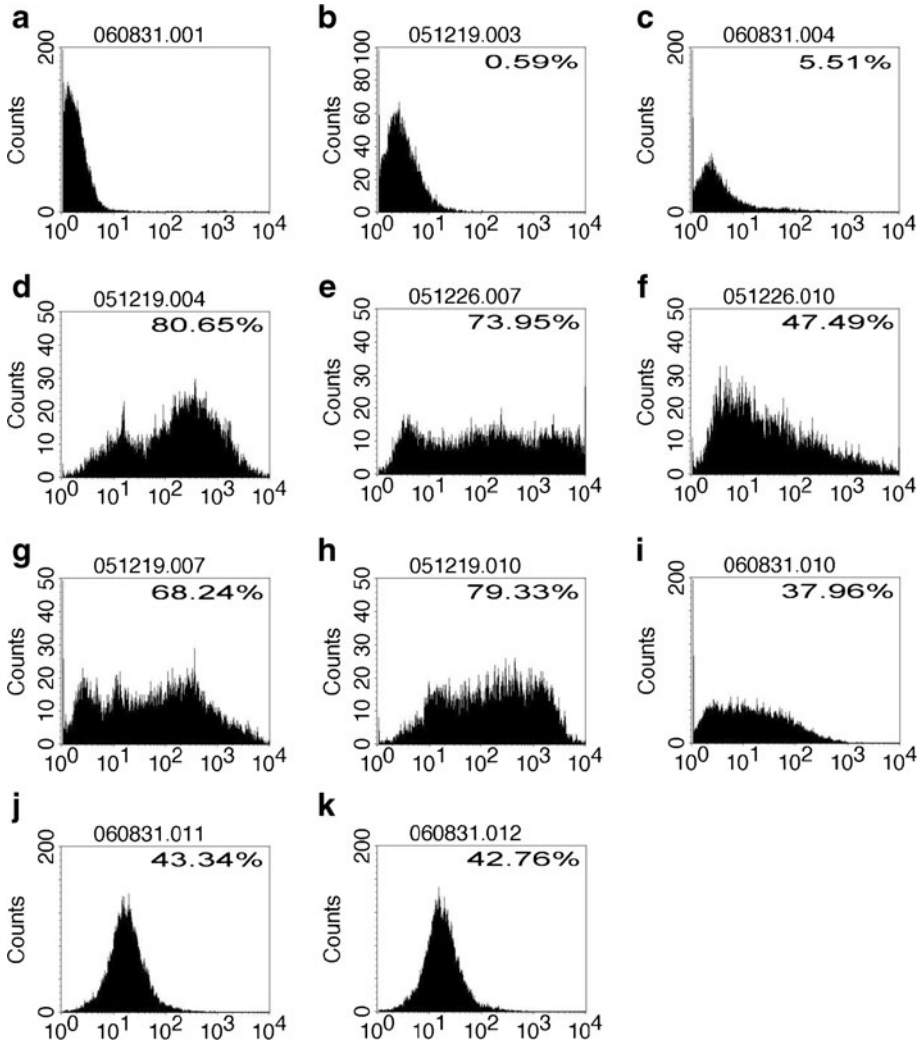

Fig. 10 FACS histograms of (**a**) control Mφ and gated cells after co-incubation of Mφ with (**b**) soluble chitosan, (**c**) soluble BSA, and BSA-loaded polymeric micro-/nanoparticles: (**d**) LCS, (**e**) HCS, (**f**) JCS, (**g**) GEL LCS, (**h**) POL LCS, (**i**) PLGA, (**j**) BCA 3 D 5, and (**k**) BCA 3 D 10.

burst release phase was observed. It is likely that the release of encapsulated BSA through the entangled long polymeric chain of HCS was too difficult. As a result, the maximum release after 14 days was lower than that obtained from the LCS microparticles (45). Chitosan of similar properties, but from different sources, clearly yielded the different release behavior of encapsulated protein. It was noticed that the chitosan composite microparticles readily suspended upon dispersion into the release medium, while the chitosan microparticles tended to form aggregates (38), likely resulted from the swelling of outer particle surface. Therefore, BSA was released from the chitosan composite microparticles more easily and in a greater amount than from the chitosan microparticles. Cross-linking with polyphosphate anions resulted in a surface coat of tripolyphosphate/chitosan complex, which could hardly be dissociated (48). Consequently, the retarded release of BSA was obtained.

Neither the spray drying process nor the compositions of chitosan microparticles deteriorated the integrity of encapsulated protein (20). In this study, there was no evidence of aggregate formation and peptide backbone clipping on the electrophoretic gel. The structural conformation of a single protein molecule can be observed within two regions of CD spectra, *i.e.* far UV (below 250 nm) and near UV (250–300 nm) which correspond to the secondary and the tertiary structure of proteins, respectively (49,50). However, the concentration of BSA recovered from the micro-/nanoparticles was too low to reveal the tertiary structure of BSA. Consequently, only investigation of the secondary structure was reported. The spectra exhibited minima at *ca.* 208 and 222 nm, which were indicative of predominantly α-helical secondary structure (50,51). The lowered molar ellipticity of BSA recovered from chitosan and chitosan composite microparticles resulted from dissolving the microparticles in an acidic solution (20). In case of the JCS microparticles, it likely contained some polarized UV light-absorbable traces, which also influenced the CD spectra of BSA recovered from the microparticles. In addition, the cationic charged groups of GEL likely interacted with the anionic charged residues of BSA, resulting in the altered conformational structure of protein.

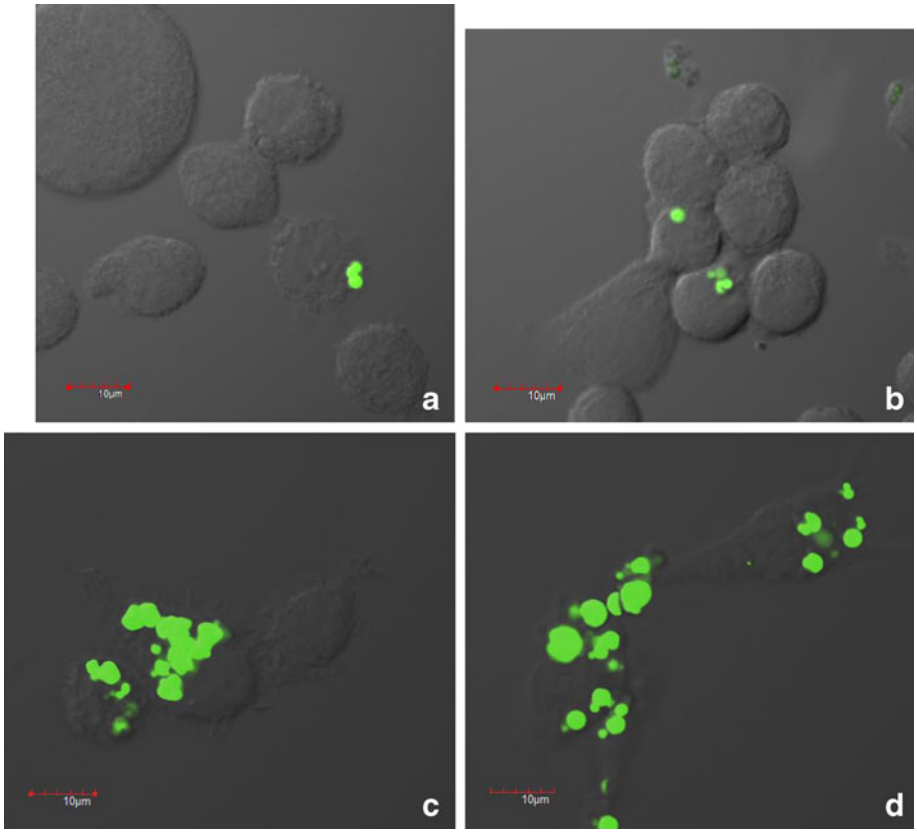

Fig. 11 Confocal laser-scanning photomicrographs of dendritic cells uptaking (**a**) LCS, (**b**) GEL LCS, and macrophages taking up (**c**) LCS, (**d**) GEL LCS microparticles (The scale bar represents 10 μm).

PLGA microparticles, with a very good appearance, were prepared by double-emulsion solvent-evaporation method. The microparticles were considered neutral. Due to the hydrophobicity and relatively high molecular weight of the polymer, the slow release of entrapped protein was obtained. The incorporated protein likely existed only in the internal aqueous phase and was subsequently entrapped *in situ* upon the particle formation. As a consequence, the deposition of protein on the particle surface was undetectable. The preparation of microparticles essentially required the use of organic solvents as well as the ultrasonic emulsification. Although they did not deteriorate the integrity of encapsulated BSA, they obviously imposed deleterious effects on the conformational structure and possibly the subsequent biological activity of encapsulated proteins (15–18).

BCA micro-/nanoparticles were prepared by anionic polymerization in aqueous media. The reaction could be initiated *via* anions, weak bases, or any nucleophilic group-containing compounds (52,53). Indeed, alkylcyanoacrylates were able to polymerize extremely rapidly in the presence of moisture or traces of basic compounds (52). The polymerization medium was thus acidified in order to regulate the reaction rate, hence promoting formation of nanoparticles in stead of large unstructured agglomerates (53). The pH of the medium was generally adjusted between 2.25 and 3.50 with a strong mineral acid such as hydrochloric acid (52–54). However, some authors reported that the reaction could be well controlled at pH 1 (55). Different agents could be used to stabilize the nanoparticles. Those containing nucleophilic groups such as D could also initiate the polymerization at the same time, resulting in the formation of amphiphilic copolymers (53). They were responsible for stabilization of the nascent polymeric particles, by exposing the polysaccharide part on the nanoparticle surface in contact with the surrounded aqueous environment (53). In the absence of D, at pH 1, the proper polymerization was not initiated (55), likely due to too low concentration of the hydroxyl anions and/or the instability of the forming particles. When pH of the polymerization medium was raised to 3, the hydroxyl anions from water were able to initiate the spontaneous polymerization more readily. It was possible that, at higher pH and/or upon incorporation of D, different particles were formed simultaneously *via* different polymerization pathways that co-existed (55). As a consequence, the smaller and more uniform-sized particles were obtained. Deposition of the neutral polysaccharide D on the particle surface (during the polymerization) resulted in the reduction of particle zeta potential. The many nucleophilic groups of proteins (amino acids) were also capable of initiating the polymerization process, leading to covalent linkages of the proteins to the forming polymer and, occasionally, an uncontrollable reaction without the formation of nanoparticles. However, the introduction of proteins after the onset/initiation of polymerization did not interfere with the reaction. The uniform nanoparticles could

then be obtained (53,56). At the polymerization pH, BSA likely exposed positive charges, which would subsequently be loaded onto the nanoparticles through the electrostatic interaction with anionic charges of the polymeric nanoparticles. Consequently, the zeta potential of particles was reduced or even turned positive in case of the polymerization at pH 1. In addition, deposition of D on the particle surface possibly interfered with the sorption of BSA, leading to the reduction of protein entrapment efficiency. The release of BSA was then rapid and controlled *via* desorption and diffusion characteristics in the releasing medium (57). The α-helical conformational change of the protein structure was noticed, probably resulted from the electrostatic interaction between BSA and the nanoparticles.

Chitosan was considered as a safe material (58). It was found that varying the polymer molecular weight did not exhibit a significant effect on the cytotoxicity of microparticles (59). Incorporation of the excipients into the chitosan microparticles did not change the influence on the cell viability significantly, except that of EUD, which was obviously more toxic to the cells. The hydrophobic side chains, *i.e.* butyl methacrylate and methyl methacrylate, of the amphiphilic polymethacrylate were reported to involve the formation of discrete nanosized pores, leading to colloid-osmotic lysis of red blood cells (60). Furthermore, the polymethacrylates with ammonium functionality might have specific interactions with phosphate head groups of membrane lipids, possibly by combination of electrostatic interactions and hydrogen bonding, which was also expected to have an important role in the pore formation (60). It was then possible that EUD produced pores in the cell membranes, leading to an influx of small solutes into the cells and subsequent rupture or destabilization of the cells. The cross-linked chitosan microparticles were relatively toxic to the cells. Some residual amounts of polyphosphate anions likely disturbed the buffering system of cell culture. Among the investigated polymeric micro-/nanoparticles, PLGA microparticles were the most cytocompatible. BCA micro-/nanoparticles were evidently toxic to the cells. The nanoparticles were degraded mainly by enzymatic hydrolysis of the ester bonds of the alkyl side chain, resulting in the formation of alkyl alcohol and poly(cyanoacrylic acid) (52,53,57). The cytotoxicity was likely caused by the local release of these degradation products, since a correlation of toxicity and degradation rate of the polymers was observed (52,57). Co-polymerization of the stabilizing polysaccharide with the polymerizing nanoparticles likely delayed the degradation rate of BCA micro-/nanoparticles. As a consequence, the lower cytotoxicity of stabilized nanoparticles was noticed. The micro-/nanoparticles polymerized at pH3 possessed a lower polydispersity index than those polymerized at pH 1, indicating more uniform particles and/or complete polymerization. This likely resulted in the slower degradation and hence the lower cytotoxicity of the micro-/nanoparticles produced at higher pH. Additionally, it was noticed that Mϕ seemed to be more sensitive to the micro-/nanoparticles than DC, probably due to higher uptake capacity of Mϕ, which was apparent in the following section.

The particulate carriers for delivery of an antigenic protein with the size of less than 5 μm were efficiently taken up into the antigen presenting cells (21). The cellular uptake can be partially controlled by altering properties of the carriers, including size and surface characteristics (61,62). In terms of size, the prospective polymeric micro-/nanoparticles produced in this study were appropriate for cellular uptake into DC and Mϕ. Immature DC could internalize various forms of antigens, including exogenous solutes, particles and necrotic or apoptotic cells, through macropinocytosis, receptor-mediated endocytosis and phagocytosis (61). However, it was evident that DC was more efficient in the uptake of the microparticulate form of antigen than the soluble form. Conversely, Mϕ seemed to favor only the uptake of particulate antigens. The lower uptake of higher molecular weight chitosan microparticles resulted from their slightly larger particle size. The suitable size ranges of microparticles for the uptake into DC and Mϕ were defined as about 50 nm–5 μm (14) and 2–3 μm (63), respectively. It appeared that the cationic chitosan and the chitosan composite microparticles were particularly effective for the internalization into DC and Mϕ (21,64). The cellular uptake of microparticles was likely initiated by the strong electrostatic affinity between the positively charged microparticles and the negatively charged cell membrane (59,65), accounting for the efficient cellular uptake of cationic microparticles. Surprisingly, increasing the positive zeta potential in case of GEL LCS microparticles did not result in further increase of particle uptake. Since the process of particle internalization was initiated through the electrostatic interaction as aforementioned, the cellular uptake of neutral PLGA microparticles and anionic BCA micro-/nanoparticles was thus less efficient than that of the cationic microparticles. In this investigation, Mϕ was clearly found to possess higher uptake capacity than DC. It was conceivable that different types of antigen presenting cells favored the internalization of different forms and/or size range of microparticles and the cationic microparticles were the most favorite for the cellular uptake. Whether the efficient particle uptake would be correlated with the subsequent enhanced immune response, still remains to be investigated.

CONCLUSION

The polymeric micro-/nanoparticles, intended for cellular delivery of proteins, were successfully prepared. Three different types of polymers, *i.e.* chitosan, PLGA and BCA, representing the cationic, neutral, and anionic polymers, respectively, were selected. Chitosan microparticles were modified either by co-spray drying with the acceptable

pharmaceutical excipients or ionically cross-linking of spray-dried microparticles with the polyphosphate anions, resulting in the particles with varied physico-chemical properties and/or biological properties. The chitosan and chitosan composite microparticles were relatively non-toxic to DC and Mϕ, except the EUD composite microparticles and the cross-linked chitosan microparticles. While PLGA microparticles were considered as safe, BCA micro-/nanoparticles were found to be relatively toxic to the tested cells. Conclusively, the chitosan and the chitosan composite microparticles were efficiently internalized by both antigen presenting cells. The prospective micro-/nanoparticles will be further investigated as the potential systems for vaccine delivery.

ACKNOWLEDGMENTS AND DISCLOSURES

Financial support from the Thailand Research Funds (TRF) through the Royal Golden Jubilee PhD Program, Office of the Higher Education Commission through the National Research University Project, and the Ratchadaphiseksomphot Endowment Fund (project code HR 1166I) is gratefully acknowledged. The authors thank the Unit Cell of Immunopathological/Clinical Research in Periodontal Diseases, Faculty of Dentistry, Chulalongkorn University for the courtesy of FACS analysis. CK is grateful to Chulalongkorn University for the travel grant and allowance during his visit at Peking University, People Republic of China.

REFERENCES

1. Kumari A, Yadav SK, Yadav SC. Biodegradable polymeric nanoparticles based drug delivery systems. Colloid Surf B - Biointerfaces. 2010;75:1–18.
2. Tan ML, Choong PFM, Dass CR. Recent developments in liposomes, microparticles, and nanoparticles for protein and peptide drug delivery. Peptides. 2010;31:184–93.
3. Ataman-Önal Y, Munier S, Ganée A, Terrat C, Durand PY, Battail N, *et al.* Surfactant-free anionic PLA nanoparticles coated with HIV-1 p24 protein induced enhanced cellular and humoral immune responses in various animal models. J Control Release. 2006;112(2):175–85.
4. Cui CJ, Stevens VC, Schwendeman SP. Injectable polymer microspheres enhance immunogenicity of a contraceptive peptide vaccine. Vaccine. 2007;25(3):500–9.
5. Feng L, Qi MR, Zhou XJ, Maitani Y, Wang SC, Jiang Y, *et al.* Pharmaceutical and immunological evaluation of a single-dose hepatitis B vaccine using PLGA microspheres. J Control Release. 2006;112(1):35–42.
6. Jaganathan KS, Vyas SP. Strong systemic and mucosal immune response to surface-modified PLGA microspheres containing recombinant hepatitis B antigen administered intranasally. Vaccine. 2006;24(19):4201–11.
7. Rajkannan R, Arul V, Padma Malar EJ, Jayakumar R. Preparation, physicochemical characterization, and oral immunogenicity of Aβ (1-12), Aβ (29-40), and Aβ (1-42) loaded PLG microparticles formulations. J Pharm Sci. 2009;98(6):2027–39.
8. Damgé C, Maincent P, Ubrich N. Oral delivery of insulin associated to polymeric nanoparticles in diabetic rats. J Control Release. 2007;117(2):163–70.
9. Estevan M, Gamazo C, Martinez-Galen F, Irache JM. Stability of poly(ε-caprolactone) microparticles containing *Brucella ovis* antigens as a vaccine delivery system against brucellosis. AAPS PharmSciTech. 2008;9(4):1063–9.
10. Sonaje K, Italia JL, Sharma G, Bhardwaj V, Tikoo K, Ravi Kumar MNV. Development of biodegradable nanoparticles for oral delivery of ellagic acid and evaluation of their antioxidant efficacy against cyclosporine A-induced nephrotoxicity in rats. Pharm Res. 2007;24(5):899–908.
11. Arias JL, Gallardo V, Ruiz MA, Delgado AV. Ftorafur loading and controlled release from poly(ethyl-2-cyanoacrylate) and poly (butylcyanoacrylate) nanospheres. Int J Pharm. 2007;337(1–2):282–90.
12. Miyazaki S, Takahashi A, Kubo W, Bachynsky J, Löbenberg R. Poly n-butylcyanoacrylate (PNBCA) nanocapsules as a carrier for NSAIDs: *in vitro* release and *in vivo* skin penetration. J Pharm Pharmaceut Sci. 2003;6(2):240–5.
13. Ren F, Chen R, Wang Y, Sun Y, Jiand Y, Li G. Paclitaxel-loaded poly(*n*-butylcyanoacrylate) nanoparticle delivery system to overcome multidrug resistance in ovarian cancer. Pharm Res. 2011;28(4):897–907.
14. de Koker S, Lambrecht BN, Willart MA, van Kooyk Y, Grooten J, Vervaet C, *et al.* Designing polymeric particles for antigen delivery. Chem Soc Rev. 2011;40:320–39.
15. Cegnar M, Kos J, Kristl J. Cystatin incorporated in poly(lactide-co-glycolide) nanoparticles: development and fundamental studies on preservation of its activity. Eur J Pharm Sci. 2004;22(5):357–64.
16. Sturesson C, Carlfors J. Incorporation of protein in PLG-microspheres with retention of bioactivity. J Control Release. 2000; 67(2–3):171–8.
17. van de Weert M, Hoechstetter J, Hennink WE, Crommelin DJA. The effect of a water/organic solvent interface on the structural stability of lysozyme. J Control Release. 2000;68:351–9.
18. Wei G, Lu LF, Lu WY. Stabilization of recombinant human growth hormone against emulsification-induced aggregation by Pluronic surfactants during microencapsulation. Int J Pharm. 2007;338:125–32.
19. Mi FL, Tan YC, Liang HF, Sung HW. *In vivo* biocompatibility and degradability of a novel injectable-chitosan-based implant. Biomaterials. 2002;23:181–91.
20. Kusonwiriyawong C, Pichayakorn W, Lipipun V, Ritthidej GC. Retained integrity of protein encapsulated in spray-dried chitosan microparticles. J Microencapsul. 2009;26(2):111–21.
21. O'Hagan DT, Singh M, Ulmer JB. Microparticle-based technologies for vaccines. Methods. 2006;40:10–9.
22. Xiang SD, Scholzen A, Minigo G, David C, Apostolopoulos V, Mottram PL, *et al.* Pathogen recognition and development of particulate vaccines: does size matter? Methods. 2006;40:1–9.
23. Bramwell VW, Perrie Y. Particulate delivery systems for vaccines: what can we expect? J Pharm Pharmacol. 2006;58:717–28.
24. Rice-Ficht AC, Arenas-Gamboa AM, Kahl-McDonagh MM, Ficht TA. Polymeric particles in vaccine delivery. Curr Opin Microbiol. 2010;13:106–12.
25. Zimmerman I. Possibilities and limitations of laser light scattering techniques for particle size analysis. In: Müller RH, Mehnert W, editors. Particle and surface characterization methods. Stuttgart: Medpharm; 1997. p. 19–26.
26. Bradford MM. A rapid and sensitive method for the quantitation of microgram quantities of protein utilizing the principle of protein-dye binding. Anal Biochem. 1976;72(1–2):248–54.
27. Amidi M, Mastrobattista E, Jiskoot W, Hennink WE. Chitosan-based delivery systems for protein therapeutics and antigens. Adv Drug Deliv Rev. 2010;62:59–82.

28. Barbour EK, Abdelnour A, Jirjis F, Faroon O, Farran MT. Evaluation of 12 stabilizers in a developed attenuated *Salmonella* Enteritidis vaccine. Vaccine. 2002;20(17–18):2249–53.
29. Kissmann J, Ausar SF, Rudolph A, Braun C, Cape SP, Sievers RE, *et al.* Stabilization of measles virus for vaccine formulation. Hum Vaccines. 2008;4(5):350–9.
30. Ohtake S, Martin RA, Saxena A, Lechuga-Ballesteros D, Santiago AE, Barry EM, *et al.* Formulation and stabilization of *Francisella tularensis* live vaccine strain. J Pharm Sci. 2011;100(8):3076–87.
31. Sarkar J, Sreenivasa BP, Singh RP, Dhar P, Bandyopadhyay SK. Comparative efficacy of various chemical stabilizers on the thermostability of a live-attenuated *peste des petits ruminants* (PPR) vaccine. Vaccine. 2003;21(32):4728–35.
32. Srirangsan P, Kawai K, Hamada-Sato N, Watanabe M, Suzuki T. Stabilizing effects of sucrose-polymer formulations on the activities of freeze-dried enzyme mixtures of alkaline phosphatase, nucleoside phosphorylase and xanthine oxidase. Food Chem. 2011;125:1188–93.
33. Thyagarajapuram N, Olsen D, Middaugh CR. Stabilization of proteins by recombinant human gelatins. J Pharm Sci. 2007;96(12):3304–15.
34. Thyagarajapuram N, Olsen D, Middaugh CR. The structure, stability and complex behavior of recombinant human gelatins. J Pharm Sci. 2007;96(12):3363–78.
35. Ameri M, Maa YF. Spray drying of biopharmaceuticals: stability and process considerations. Drying Technol. 2006;24:763–8.
36. Elversson J, Millqvist-Fureby A. *In situ* coating – an approach for particle modification and encapsulation of proteins during spray-drying. Int J Pharm. 2006;323:52–63.
37. Westerink MAJ, Smithson SL, Srivastava N, Blonder J, Coeshott C, Rosenthal GJ. ProJuvant™ (Pluronic F 127®/chitosan) enhances the immune response to intranasally administered tetanus toxoid. Vaccine. 2002;20:711–23.
38. Kang ML, Jiang HL, Kang SG, Guo DD, Lee DY, Cho CS, *et al.* Pluronic® F 127 enhances the effect as an adjuvant of chitosan microspheres in the intranasal delivery of *Bordetella bronchiseptica* antigens containing dermonecrotoxin. Vaccine. 2007;25:4602–10.
39. Collett JH, Weller PJ. Poloxamer. In: Wade A, Weller PJ, editors. Handbook of pharmaceutical excipients. Washington: American Pharmaceutical Association; 1994. p. 352–4.
40. Kusonwiriyawong C, van de Wetering P, Hubbell JA, Merkle HP, Walter E. Evaluation of pH-dependent membrane-disruptive properties of poly(acrylic acid) derived polymers. Eur J Pharm Biopharm. 2003;56:237–46.
41. Kohane DS, Anderson DG, Yu C, Langer R. pH-triggered release of macromolecules from spray-dried polymethacrylate microparticles. Pharm Res. 2003;20(10):1533–8.
42. Haining WN, Anderson DG, Little SR, von Bergwelt-Baildon MS, Cardoso AA, Alves P, *et al.* pH-triggered microparticles for peptide vaccination. J Immunol. 2004;173:2578–85.
43. Shu XZ, Zhu KJ. Chitosan/gelatin microspheres prepared by modified emulsification and ionotropic gelation. J Microencapsul. 2001;18(2):237–45.
44. Ko JA, Park HJ, Hwang SJ, Park JB, Lee JS. Preparation and characterization of chitosan microparticles intended for controlled drug delivery. Int J Pharm. 2002;249:165–74.
45. Gan Q, Wang T. Chitosan nanoparticle as protein delivery carrier – systematic examination of fabrication conditions for efficient loading and release. Colloid Surf B – Biointerfaces. 2007;59:24–34.
46. Malamud D, Drysdale JW. Isoelectric points of proteins: a table. Anal Biochem. 1978;86:620–47.
47. Righetti PG, Caravaggio T. Isoelectric points and molecular weights of proteins: a table. J Chromatog A. 1976;127:1–28.
48. Shu XZ, Zhu KJ. Controlled drug release properties of ionically cross-linked chitosan beads: the influence of anion structure. Int J Pharm. 2002;233:217–25.
49. Kelly SM, Price NC. The application of circular dichroism to studies of protein folding and unfolding. Biochim Biophys Acta. 1997;1338:161–85.
50. Sreerama N, Woody RW. Circular dichroism of peptides and proteins. In: Berova N, Nakanishi K, Woody RW, editors. Circular dichroism: principles and applications. New York: Wiley-VCH; 2000. p. 601–20.
51. Pelton JT, McLean LR. Spectroscopic methods for analysis of protein secondary structure. Anal Biochem. 2000;277:167–76.
52. Vauthier C, Dubernet C, Fattal E, Pinto-Alphandary H, Couvreur P. Poly(alkylcyanoacrylates) as biodegradable materials for biomedical applications. Adv Drug Deliv Rev. 2003;55:519–48.
53. Vauthier C, Labarre D, Ponchel G. Design aspects of poly(alkylcyanoacrylate) nanoparticles for drug delivery. J Drug Target. 2007;15(10):641–63.
54. Behan N, Birkinshaw C, Clarke N. Poly *n*-butyl cyanoacrylate nanoparticles: a mechanistic study of polymerizaiton and particle formation. Biomaterials. 2001;22:1335–44.
55. Chauvierre C, Labarre D, Couvreur P, Vauthier C. Plug-in spectrometry with optical fibers as a novel analytical tool for nanoparticles technology: application to the investigation of the emulsion polymerization of the alkylcyanoacrylate. J Nanopart Res. 2003;5:365–71.
56. Behan N, Birkinshaw C. Preparation of poly(butyl cyanoacrylate) nanoparticles by aqueous dispersion polymerization in the presence of insulin. Macromol Rapid Commun. 2001;22:41–3.
57. Graf A, McDowell A, Rades T. Poly(alkylcyanoacrylate) nanoparticles for enhanced delivery of therapeutics – is there real potential? Expert Opin Drug Deliv. 2009;6(4):371–87.
58. Illum L. Chitosan and its use as a pharmaceutical excipient. Pharm Res. 1998;15(9):1326–31.
59. Huang M, Khor E, Lim LY. Uptake and cytotoxicity of chitosan molecules and nanoparticles: effects of molecular weight and degree of deacetylation. Pharm Res. 2004;21(2):344–53.
60. Sovadinova I, Palermo EF, Huang R, Thoma LM, Kuroda K. Mechanism of polymer-induced hemolysis: nanosized pore formation and osmotic lysis. Biomacromolecules. 2011;12(1):260–8.
61. Reddy ST, Swartz MA, Hubbell JA. Targeting dendritic cells with biomaterials: developing the next generation of vaccines. Trends Immunol. 2006;27(12):573–9.
62. Alexis F, Pridgen E, Molnar LK, Farokhzad OC. Factors affecting the clearance and biodistribution of polymeric nanoparticles. Mol Pharm. 2008;5(4):505–15.
63. Champion JA, Walker A, Mitragotri S. Role of particle size in phagocytosis of polymeric microspheres. Pharm Res. 2008;25(8):1815–21.
64. Thiele L, Merkle HP, Walter E. Phagocytosis and phagosomal fate of surface-modified microparticles in dendritic cells and macrophages. Pharm Res. 2003;20(2):221–8.
65. He C, Hu Y, Yin L, Tang C, Yin C. Effects of particle size and surface charge on cellular uptake and biodistribution of polymeric nanoparticles. Biomaterials. 2010;31:3657–66.